Correlations in disordered crystals and diffuse scattering of x rays or neutrons

S. Dietrich* and W. Fenzl
Sektion Physik der Ludwig-Maximilians Universität München, Geschwister-Scholl Platz 1, D-8000 München 22, Federal Republic of Germany
(Received 8 June 1988)

The scattering cross section for diffuse scattering of x rays or neutrons from disordered crystals is expressed systematically in terms of density-correlation functions by using a cumulant expansion. This approach allows one to distinguish between contributions owing to pair-, three-, and higher-order correlations of the defects; the latter ones enter even within the first Born approximation due to the nonlinear dependence of the scattering amplitude on the lattice displacements. The terms involving even and odd correlation functions, respectively, can be classified according to their inversion symmetry properties. This analysis is applied to x-ray scattering data obtained from niobium-molybdenum alloys loaded with hydrogen. Furthermore, we propose how to test, on the basis of the scattering data alone, approximation schemes for the three-point correlation function, such as, e.g., the Kirkwood superposition principle.

I. INTRODUCTION

Interstitial defects in crystals occur either as contaminations[1-3] or they are dissolved like hydrogen atoms in metals.[4] In both cases the knowledge of the correlation functions of these defects provides a detailed insight into the interactions between them as well as into their thermal behavior. This becomes particularly interesting when these interstitial defects undergo cooperative phenomena which are induced through effective interactions mediated by the host lattice. The phase transitions of hydrogen atoms dissolved in certain metals are well-known examples thereof.[4]

X-ray and neutron scattering are standard techniques for such structural investigations. Since in the case under study the single scattering cross section is small *a fortiori* multiple scattering is negligible and the scattered intensity is proportional to the Fourier transformed pair correlation function of the atoms in space and time.[5] In general the atoms are displaced from their ideal lattice positions so that this Fourier transform is a nonlinear function of the occupation numbers $\{\tau_a=0,1\}$ of the interstitial sites labeled by $a=1,\ldots,N_H$. Therefore the scattered intensity depends in a complicated way on the whole set of the correlation functions

$$G^{(m)}=\left\langle \prod_{i=1}^{m} \tau_{a_i} \right\rangle \quad (m=1,\ldots,\infty)$$

mentioned above.

The same situation arises in binary alloys. There, in the particular case that the alloy components have similar atomic sizes, these displacements are small so that in a first approximation the scattered intensity depends linearly on $G^{(2)}$ known as short-range order scattering.[6-8] But even for those favorable alloys like CuZn the different atomic sizes of the alloy components induce long-ranged displacement fields and introduce important nonlinearities. Therefore *a fortiori* the general case of binary alloys requires considerations as for interstitial defects. A method to analyze the diffuse scattering including the distortion-induced scattering was developed by Borie and Sparks[8] and applied extensively by, among others, Cohen and co-workers.[7] A corresponding analysis based on results of the present paper is presented in Ref. 9.

It is well known[10-12] that interstitial defects cause a dilation of the host lattice resulting in a shift of the position of the Bragg peaks. The magnitude of this shift is determined by the *mean concentration* $G^{(1)}\equiv c$. The *fluctuations* of the defect configurations lead to local distortions around the dilated mean lattice. This causes the so-called Huang diffuse scattering around the shifted Bragg peaks.[13-20] Based on truncations Krivoglaz[14] found that this diffuse scattering intensity is proportional to the product of the Fourier transform of $G^{(2)}$ and the absolute square of the Fourier transform of the displacement field of a single defect. He also discusses to some extent within this approximation scheme the influence of $G^{(3)}$.

Instead, in this paper we employ a cumulant expansion of the structure factor.[21-23] This approach enables us to discuss in a clear and systematic way how the whole hierarchy of correlation functions enters the scattering intensity. It allows one also to judge the validity of Krivoglaz's original Huang diffuse scattering formula. In particular one obtains the dependence of the Debye-Waller factor on the correlation functions of the defects.

In Sec. II we derive the general expression for the cross section and we discuss in detail the scattering process at the host lattice. Furthermore we show how the experimentally determined function $G^{(2)}$ can be used in order to test theoretical approximation schemes for $G^{(3)}$. The scattering at the interstitials themselves and the cross term are analyzed in Sec. III. In Sec. IV we apply our results to x-ray scattering data obtained from niobium-molybdenum alloys loaded with deuterium. Section V gives a summary and conclusion. In Appendix A we provide crude approximations for $G^{(2)}$, $G^{(3)}$, and $G^{(4)}$ in order to be able to obtain in Appendix B estimates for vari-

ous contributions to the cross section. In Appendix C we compare the information about $G^{(3)}$ following from the pressure dependence of $G^{(2)}$ with the one, which can be extracted from the antisymmetric part of the Huang diffuse scattering.

II. THE SCATTERING CROSS SECTION

A. Cumulant expansion

Each configuration of the sample is described by the set of host-lattice sites $\{\mathbf{R}_m | m=1,\ldots,N_L\}$ and the set of interstitial sites $\{\mathbf{S}_a | a=1,\ldots,N_H\}$. Every site of the host lattice is assumed to be occupied by atoms, whereas the interstitial sites are either occupied ($\tau_a=1$) by a defect or they are unoccupied ($\tau_a=0$). We decompose the vectors $\mathbf{R}_m$ and $\mathbf{S}_a$ into their thermal mean values and their displacements, respectively,

$$\mathbf{R}_m(t)=\mathbf{R}_m+\mathbf{u}_m(t) \tag{2.1}$$

and

$$\mathbf{S}_a(t)=\mathbf{S}_a+\mathbf{v}_a(t) \tag{2.2}$$

with

$$\langle \mathbf{u}_m(t)\rangle=0 \tag{2.3}$$

and

$$\langle \mathbf{v}_a(t)\rangle=0\ ; \tag{2.4}$$

t denotes the time dependence of the corresponding quantities. $\{\mathbf{R}_m\}$ and $\{\mathbf{S}_a\}$ form regular lattice structures which differ from those of the sample without defects only by a homogeneous dilation of the lattice constant depending on the defect concentration $c=\langle \tau_a \rangle$. Therefore $\{\mathbf{R}_m\}$ gives rise to Bragg peaks which are shifted compared to the unperturbed crystal, whereas $\{\mathbf{u}_m(t)\}$ and $\{\mathbf{v}_a(t)\}$ cause the aforementioned diffuse scattering intensity which we study in the following.

In order to avoid clumsy notation we consider a host crystal which consists of only a single type of atoms. But our conclusions can easily be generalized to more complicated situations. The above description of the sample is applicable both to gases dissolved in metals and to superionic conductors.[24–27] There are also no principal differences to the case of substitutional alloys.

According to van Hove[5,28–30] the scattering cross section for the scattering of x rays or neutrons from condensed matter is proportional to a dynamic structure factor $S(\mathbf{K},\omega)$,

$$d^2\sigma/(d\Omega\, d\omega)=AS(\mathbf{K},\omega) \tag{2.5}$$

with

$$S(\mathbf{K},\omega)=(2\pi)^{-1}\int_{-\infty}^{+\infty} dt\, e^{i\omega t}\langle \rho(\mathbf{K},t)\rho^*(\mathbf{K},0)\rangle \tag{2.6}$$

and

$$A=(e^2/mc^2)^2(K_f/K_i)(\mathbf{s}_i\mathbf{s}_f)^2 \tag{2.7}$$

for x rays and

$$A=(K_f/K_i) \tag{2.8}$$

for neutrons, respectively, $K=|\mathbf{K}|$ and $\mathbf{s}$ is the polarization vector for the electromagnetic waves. $\mathbf{K}$ and ω correspond to the momentum and energy transfer between the initial and final state of the scattered waves,

$$\mathbf{K}=\mathbf{K}_i-\mathbf{K}_f \tag{2.9}$$

and

$$\omega=\omega_i-\omega_f\ , \tag{2.10}$$

$$\rho(\mathbf{K},t)=\sum_n f_n(\mathbf{K},t)\exp[i\mathbf{K}\cdot\mathbf{R}_n(t)] \tag{2.11}$$

is the scattering amplitude of the electrons and nuclei, respectively. In neutron scattering f is a coherent scattering length, whereas in x-ray scattering f is the atomic form amplitude

$$f(\mathbf{K})=\int d^3R\, e^{i\mathbf{K}\cdot\mathbf{R}}\rho_e(R)=f(-\mathbf{K})\equiv f\ , \tag{2.12}$$

the Fourier transform of the electron density of the regular lattice atoms or the defects. Since the defects will modify the electron density of the host atoms, for x rays $f(\mathbf{K})$ depends also on the defect concentration.

We consider only coherent scattering processes and do not discuss incoherent or spin-dependent scattering of neutrons or Compton scattering of x rays.

With our description of the sample as given above one obtains

$$\rho(\mathbf{K},t)=f_{\rm at}\sum_m e^{i\mathbf{K}\cdot[\mathbf{R}_m+\mathbf{u}_m(t)]}+f_{\rm def}\sum_a \tau_a(t)e^{i\mathbf{K}\cdot[\mathbf{S}_a+\mathbf{v}_a(t)]}\ . \tag{2.13}$$

Here $f_{\rm at}$ denotes the scattering length or atomic form amplitude of the atoms which form a completely occupied lattice hosting interstitial defects with scattering length or atomic form amplitude $f_{\rm def}$.

According to Eqs. (2.6) and (2.13) the structure factor separates into three distinct contributions,

$$S(\mathbf{K},\omega)=S_1(\mathbf{K},\omega)+S_2(\mathbf{K},\omega)+S_3(\mathbf{K},\omega) \tag{2.14}$$

with

$$S_1(\mathbf{K},\omega)=|f_{\rm at}|^2\sum_{m,n} e^{i\mathbf{K}\cdot(\mathbf{R}_m-\mathbf{R}_n)}(2\pi)^{-1}\int_{-\infty}^{+\infty} dt\, e^{i\omega t}\langle e^{i\mathbf{K}\cdot[\mathbf{u}_m(t)-\mathbf{u}_n(0)]}\rangle\ , \tag{2.15}$$

$$S_2(\mathbf{K},\omega)=|f_{\rm def}|^2\sum_{a,b} e^{i\mathbf{K}\cdot(\mathbf{S}_a-\mathbf{S}_b)}(2\pi)^{-1}\int_{-\infty}^{+\infty} dt\, e^{i\omega t}\langle \tau_a(t)\tau_b(0)e^{i\mathbf{K}\cdot[\mathbf{v}_a(t)-\mathbf{v}_b(0)]}\rangle\ , \tag{2.16}$$

and

$$S_3(\mathbf{K},\omega)=2\,\mathrm{Re}\left[f_{\mathrm{at}}f^{*}_{\mathrm{def}}\sum_{m,a}e^{i\mathbf{K}\cdot(\mathbf{R}_m-\mathbf{S}_a)}(2\pi)^{-1}\int_{-\infty}^{+\infty}dt\,e^{i\omega t}\langle\tau_a(0)e^{i\mathbf{K}\cdot[\mathbf{u}_m(t)-\mathbf{v}_a(0)]}\rangle\right]. \tag{2.17}$$

S_1 represents the scattering at the host lattice, S_2 the scattering at the defects, and S_3 is the cross term with contributions from both. The next step requires the evaluation of the thermal averages $\langle\ \rangle$ in Eqs. (2.15)–(2.17). For hydrogen in metals it is known[25] that the dissolved defects are in thermal equilibrium with the host lattice. Therefore, in this case the correlation functions are those following from equilibrium statistical mechanics. It is important to note that owing to the well-known relation between a lattice gas and a binary alloy Eqs. (2.15)–(2.17) also describe the scattering from a two-component alloy like CuZn. For more details see Refs. 6 and 9.

In order to be able to draw transparent conclusions about the system under consideration, one aims for expressing these averages in terms of the correlation functions $G^{(m)}$ which have been defined in the Introduction. Then the scattered intensity can be interpreted in terms of the Fourier transform of the functions $G^{(m)}$.

Two important systems—irradiated crystals and gases dissolved in metals—offer the opportunity to perform scattering experiments with and without defects. By taking the difference between these two scattered intensities with appropriate corrections[31] one obtains that part of the diffuse scattering which is caused by the defects alone. This yields the desired information about the correlations of the defects.

In the conventional approach[8,14] the displacement fields $\mathbf{u}_m$ and $\mathbf{v}_a$ in each cell and for every configuration contributing to the thermal-averaging procedure are assumed to be small enough so that in the expansion of the phase factors $\exp(i\mathbf{K}\cdot\mathbf{u}_m)=1+i\mathbf{K}\cdot\mathbf{u}_m+\cdots$ and likewise for $\exp(i\mathbf{K}\cdot\mathbf{v}_a)$ all nonlinear terms can be neglected. Then one takes the thermal average of this expansion. The underlying tacit assumption behind this procedure is that all those displacement configurations, for which $\mathbf{u}_m$ and $\mathbf{v}_a$ are not small, are strongly suppressed by their corresponding Boltzmann factor. However, in general this assumption is not justified. For that reason we take a different approach.

The idea is as follows. Consider a stochastic variable X and its generating function

$$g(\lambda)=\langle\exp\lambda X\rangle\ . \tag{2.18}$$

Here λ is a parameter and $\langle\ \rangle$ means the average taken with the probability distribution $P(X)$ for X. Following the *conventional approach* described above one writes

$$g(\lambda)=\sum_{n=0}^{\infty}(\lambda^n/n!)\langle X^n\rangle\ . \tag{2.19}$$

In general Eq. (2.19) is not valid because for sufficiently large n the moments fail to exist if $P(X)$ decays as a power law for large X. Thus a necessary condition for Eq. (2.19) is that $P(X)$ decays exponentially for large X. On the other hand, in the *cumulant expansion*[21] the function $g(\lambda)$ is written as

$$g(\lambda)=\exp[h(\lambda)] \tag{2.20}$$

with

$$h(\lambda)=\sum_{n=1}^{\infty}(\lambda^n/n!)\kappa_n\ . \tag{2.21}$$

Due to the normalization of $P(X)$ one has $g(0)=1$ and therefore $h(0)=0$. The derivatives of $h(\lambda)$ at $\lambda=0$ define the cumulants $\kappa_n=\langle X^n\rangle_c$. The first few of them are

$$\kappa_1=\langle X\rangle\ , \tag{2.22}$$

$$\kappa_2=\langle X^2\rangle-\langle X\rangle^2=\langle X^2\rangle-\kappa_1\ , \tag{2.23}$$

$$\kappa_3=\langle X^3\rangle-3\langle X\rangle\langle X^2\rangle+2\langle X\rangle^3$$
$$=\langle X^3\rangle-3\kappa_1\kappa_2-\kappa_1^3\ , \tag{2.24}$$

and

$$\kappa_4=\langle X^4\rangle-4\langle X^3\rangle\langle X\rangle-3\langle X^2\rangle^2$$
$$+12\langle X^2\rangle\langle X\rangle^2-6\langle X\rangle^4$$
$$=\langle X^4\rangle-4\kappa_1\kappa_3-6\kappa_1^2\kappa_2-3\kappa_2^2-\kappa_1^4\ . \tag{2.25}$$

Notice that κ_n is determined by $\langle X^n\rangle$ and all cumulants κ_i with $i\le n-1$. The main advantage of the cumulant expansion becomes obvious if we consider for the moment $P(X)$ to be Gaussian. In this case $\kappa_n=0$ for $n\ge 3$ and the sum in Eq. (2.21) reduces to two terms, whereas the sum in Eq. (2.19) still consists of an *infinite* number of terms. The cumulant expansion sums them up to give

$$g(\lambda)=\exp(\lambda\kappa_1+\lambda^2\kappa_2/2),\quad P(X)\ \text{Gaussian}\ . \tag{2.26}$$

For a general distribution $P(X)$, both sums [Eqs. (2.19) and (2.21)] will consist of an infinite number of terms. But the cumulant expansion [Eq. (2.21)] converges much faster because due to Eq. (2.20) the expansion in moments [Eq. (2.19)] has partially been summed up.

Besides these mathematical merits the cumulant expansion allows one to judge the range of validity for neglecting higher-order terms on the basis of physical arguments. In general the higher-order cumulants, i.e., κ_n with $n\ge 3$, are small if there are no strong fluctuations in the system. This is the case as long as one is far away from any critical points of the system. Hydrogen atoms dissolved in metals do have a critical point between gas- and liquidlike phases (α-α' phase transition[4]) but due to the long-ranged interactions between the interstitials, this critical point is a classical one with mean-field-type critical exponents. Therefore in this case the cumulant expansion should remain meaningful. It will break down, however, near a continuous order-disorder transition in a binary alloy. Note, however, that even in the absence of strong fluctuations the higher cumulants may be still significant owing to special properties of the stochastic variable X [see Eqs. (A7) and (A8)].

In order to be able to apply the cumulant expansion to Eq. (2.15) we use the expression for two stochastic variables:[21]

$$\langle \exp(X_1+X_2)\rangle = \langle \exp X_1\rangle \langle \exp X_2\rangle \exp[\langle X_1X_2\rangle_c + \tfrac{1}{2}\langle X_1^2X_2 + X_1X_2^2\rangle_c + \tfrac{1}{4}\langle X_1^2X_2^2\rangle_c + \tfrac{1}{6}\langle X_1^3X_2 + X_1X_2^3\rangle_c + \cdots] , \tag{2.27}$$

where in general

$$\langle X_1X_2\rangle_c = \langle X_1X_2\rangle - \langle X_1\rangle\langle X_2\rangle , \tag{2.28}$$

$$\langle X_1X_2X_3\rangle_c = \langle X_1X_2X_3\rangle - \langle X_1\rangle\langle X_2X_3\rangle - \langle X_2\rangle\langle X_1X_3\rangle - \langle X_3\rangle\langle X_1X_2\rangle + 2\langle X_1\rangle\langle X_2\rangle\langle X_3\rangle , \tag{2.29}$$

and for $\langle X_i\rangle = 0$, $i = 1, \ldots, 4$,

$$\langle X_1X_2X_3X_4\rangle_c = \langle X_1X_2X_3X_4\rangle - \langle X_1X_2\rangle\langle X_3X_4\rangle - \langle X_1X_4\rangle\langle X_2X_3\rangle - \langle X_1X_3\rangle\langle X_2X_4\rangle . \tag{2.30}$$

For $X_i = X$ Eqs. (2.28)–(2.30) reduce to Eqs. (2.22)–(2.25). In general one has $\langle \exp \sum_i X_i\rangle = \exp\langle \exp(\sum_i X_i) - 1\rangle_c$, where $\langle\ \rangle_c$ means that the exponential function in it is expanded and each product is averaged by the cumulant average.[21] Note that the cumulant expansion in Eq. (2.27) has been rearranged in such a way that, in accordance with Eqs. (2.28)–(2.30), the third exponential factor on the right-hand side carries contributions only from those correlations, which arise solely due to the statistical dependence of X_1 and X_2.

Thus we obtain [see Eqs. (2.15) and (2.3)]

$$\begin{aligned}\langle e^{i\mathbf{K}\cdot[\mathbf{u}_m(t)-\mathbf{u}_n(0)]}\rangle = \langle e^{i\mathbf{K}\cdot\mathbf{u}_m(t)}\rangle\langle e^{-i\mathbf{K}\cdot\mathbf{u}_n(0)}\rangle \\ \times \exp\{\langle[\mathbf{K}\cdot\mathbf{u}_m(t)][\mathbf{K}\cdot\mathbf{u}_n(0)]\rangle_c + i\langle[\mathbf{K}\cdot\mathbf{u}_m(t)]^2[\mathbf{K}\cdot\mathbf{u}_n(0)]\rangle_c \\ + \tfrac{1}{4}\langle[\mathbf{K}\cdot\mathbf{u}_m(t)]^2[\mathbf{K}\cdot\mathbf{u}_n(0)]^2\rangle_c - \tfrac{1}{3}\langle[\mathbf{K}\cdot\mathbf{u}_m(t)]^3[\mathbf{K}\cdot\mathbf{u}_n(0)]\rangle_c + \cdots\}\end{aligned} \tag{2.31}$$

with

$$\langle[\mathbf{K}\cdot\mathbf{u}_m(t)][\mathbf{K}\cdot\mathbf{u}_n(0)]\rangle_c = \langle[\mathbf{K}\cdot\mathbf{u}_n(t)][\mathbf{K}\cdot\mathbf{u}_m(0)]\rangle_c , \tag{2.32}$$

$$\langle[\mathbf{K}\cdot\mathbf{u}_m(t)]^2[\mathbf{K}\cdot\mathbf{u}_n(0)]\rangle_c = -\langle[\mathbf{K}\cdot\mathbf{u}_n(t)]^2[\mathbf{K}\cdot\mathbf{u}_m(0)]\rangle_c , \tag{2.33}$$

$$\langle[\mathbf{K}\cdot\mathbf{u}_m(t)]^2[\mathbf{K}\cdot\mathbf{u}_n(0)]^2\rangle_c = \langle[\mathbf{K}\cdot\mathbf{u}_n(t)]^2[\mathbf{K}\cdot\mathbf{u}_m(0)]^2\rangle_c , \tag{2.34}$$

and

$$\langle[\mathbf{K}\cdot\mathbf{u}_m(t)]^3[\mathbf{K}\cdot\mathbf{u}_n(0)]\rangle_c = \langle[\mathbf{K}\cdot\mathbf{u}_n(t)]^3[\mathbf{K}\cdot\mathbf{u}_m(0)]\rangle_c . \tag{2.35}$$

The antisymmetry of the expressions in Eq. (2.33) and the symmetry of the expressions in Eq. (2.35) are due to the inversion symmetry of the lattices $\{\mathbf{R}_m\}$ and $\{\mathbf{S}_a\}$, respectively, and they reflect the antisymmetry of the displacement field $\mathbf{T}^{(1)}(\mathbf{R}_m - \mathbf{S}_a)$ of a single interstitial defect [cf. Eq. (2.51)]; for a particular example see also Eqs. (2.61) and (B6). Analogous symmetry properties hold for higher-order displacement fields like $\mathbf{T}^{(2)}$ [cf. Eq. (2.51)]. These considerations also show that the autocorrelation functions $\langle(\mathbf{K}\cdot\mathbf{u}_m)^p\rangle$ vanish for odd p. In Eqs. (2.32)–(2.35) surface effects have been neglected so that the correlation functions are translationally invariant. For the same reason the first two terms on the right-hand side of Eq. (2.31) are spatially constant,

$$\langle e^{i\mathbf{K}\cdot\mathbf{u}_m(t)}\rangle = \langle e^{-i\mathbf{K}\cdot\mathbf{u}_n(0)}\rangle = e^{-W(\mathbf{K})} . \tag{2.36}$$

This is the well-known, *full* Debye-Waller factor, which contains contributions from both the lattice vibrations and the defect-induced displacements.[14,32] It should be pointed out that in the cumulant expansion this Debye-Waller factor is extracted always exactly even if this expansion is finally truncated [see Eq. (2.31)]. This represents a considerable advantage over the truncated conventional approach [see Eq. (2.19)], where this is not the case. $W(\mathbf{K})$ can be determined experimentally by measuring the integrated intensity of Bragg peaks which yields information about the autocorrelation functions:[33]

$$W(\mathbf{K}) = \tfrac{1}{2}\langle(\mathbf{K}\cdot\mathbf{u})^2\rangle + \tfrac{1}{24}[3\langle(\mathbf{K}\cdot\mathbf{u})^2\rangle^2 - \langle(\mathbf{K}\cdot\mathbf{u})^4\rangle] + \cdots = W(-\mathbf{K}) . \tag{2.37}$$

We apply the cumulant expansion also to the contributions S_2 and S_3 of the cross section [Eqs. (2.16) and (2.17)]. For S_3 one obtains

$$\langle \tau_a(0) e^{i\mathbf{K}\cdot[\mathbf{u}_m(t)-\mathbf{v}_a(0)]}\rangle = (\partial/\partial\lambda_a)\langle e^{\lambda_a\tau_a(0) + i\mathbf{K}\cdot[\mathbf{u}_m(t)-\mathbf{v}_a(0)]}\rangle_{|\lambda_a=0} . \tag{2.38}$$

In order to bear out explicitly the behavior of this correlation function for $|\mathbf{R}_m - \mathbf{S}_a| \to \infty$ we apply Eq. (2.27) by identifying X_1 with $\lambda_a\tau_a(0) - i\mathbf{K}\cdot\mathbf{v}_a(0)$ and X_2 with $i\mathbf{K}\cdot\mathbf{u}_m$,

$$\langle e^{\lambda_a\tau_a(0)+i\mathbf{K}\cdot[\mathbf{u}_m(t)-\mathbf{v}_a(0)]}\rangle=\langle e^{\lambda_a\tau_a(0)-i\mathbf{K}\cdot\mathbf{v}_a(0)}\rangle\langle e^{i\mathbf{K}\cdot\mathbf{u}_m(t)}\rangle\exp\{\langle[\lambda_a\tau_a(0)-i\mathbf{K}\cdot\mathbf{v}_a(0)][\mathbf{K}\cdot\mathbf{u}_m(t)]\rangle_c+\cdots\}\ . \tag{2.39}$$

The third factor on the right-hand side of Eq. (2.39) tends to 1 for $|\mathbf{R}_m-\mathbf{S}_a|\to\infty$. This corresponds to a suitable rearrangement of the cumulant series

$$\left\langle\exp\left[\sum_i X_i\right]\right\rangle=\exp\left[\left\langle\exp\left[\sum_i X_i\right]-1\right\rangle_c\right]\ .$$

Similarly one finds for the contribution entering S_2

$$\langle\tau_a(t)\tau_b(0)e^{i\mathbf{K}\cdot[\mathbf{v}_a(t)-\mathbf{v}_b(0)]}\rangle=(\partial^2/\partial\lambda_a\partial\lambda_b)\langle e^{[\lambda_a\tau_a(t)+i\mathbf{K}\cdot\mathbf{v}_a(t)]+[\lambda_b\tau_b(0)-i\mathbf{K}\cdot\mathbf{v}_b(0)]}\rangle_{|\lambda_a=\lambda_b=0}\ . \tag{2.40}$$

For the same purpose as above we apply Eq. (2.27) with $X_1=\lambda_a\tau_a(t)+i\mathbf{K}\cdot\mathbf{v}_a(t)$ and $X_2=\lambda_b\tau_b(0)-i\mathbf{K}\cdot\mathbf{v}_b(0)$. The resulting cumulants can be expressed again in terms of cumulants containing τ_a, $\mathbf{K}\cdot\mathbf{v}_a$, τ_b, or $\mathbf{K}\cdot\mathbf{v}_b$ as factors, because the cumulants $\langle X_1\cdots X_n\rangle_c$ are multilinear with respect to their variables $X_1,\ldots,X_n$.

For example in the case of neutron scattering at metal-hydrogen systems or at binary alloys the correlation functions in Eqs. (2.38) and (2.40) represent important contributions to the total scattering intensity. We present a detailed discussion of these terms in Sec. III. However, in the case of x-ray scattering at metal-hydrogen systems $|f_{\rm def}/f_{\rm at}|\ll 1$ so that the contributions of S_2 and S_3 to the total structure factor S are very small. Therefore in the following, Sec. II B, we focus on S_1 alone.

B. Distortion-induced scattering

Up to here we have neither made an assumption about the concentration of defects nor about the magnitude of the displacements induced by them. In order to facilitate a transparent interpretation of the cross section, we now resort to approximations concerning the contributions from various correlation functions which allow us to study the influence of the hierarchy of the correlation functions on the diffuse scattering intensity.

Since the Fourier transform of a function $F(R)=\exp[f(R)]$ cannot be expressed in closed form in terms of the Fourier transform of $f(R)$, we expand the third, exponential factor on the right-hand side of Eq. (2.31). Thus, we obtain with Eqs. (2.15), (2.31)–(2.35), and (2.36)

$$\begin{aligned}S_1(\mathbf{K},\omega)=&N_L|f_{\rm at}|^2e^{-2W(\mathbf{K})}[(2\pi)^3/V_{\rm cell}]\\&\times\Bigg[\sum_n\delta(\mathbf{K}-\mathbf{G}_n)\delta(\omega)+\sum_{i,j}K_iK_jC_{ij}^{(2)}(\mathbf{q},\omega)+i\sum_{i,j,k}K_iK_jK_kC_{ijk}^{(3)}(\mathbf{q},\omega)\\&+\sum_{i,j,k,l}K_iK_jK_kK_l\Bigg[\tfrac{1}{2}\int d\omega'\int d^3q'\,C_{ij}^{(2)}(\mathbf{q}',\omega')C_{kl}^{(2)}(\mathbf{q}-\mathbf{q}',\omega-\omega')\\&+\tfrac{1}{4}C_{ijkl}^{(4,1)}(\mathbf{q},\omega)-\tfrac{1}{3}C_{ijkl}^{(4,2)}(\mathbf{q},\omega)\Bigg]+\cdots\Bigg]\ ,\end{aligned} \tag{2.41}$$

where

$$\int d\omega=\int_{-\infty}^{+\infty}d\omega,\quad \int d^3q=[V_{\rm cell}/(2\pi)^3]\int d^3q\ .$$

$(2\pi)^3/V_{\rm cell}$ is the volume of the first Brillouin zone (1 BZ) of the host lattice. $\mathbf{G}_n$ are reciprocal lattice vectors such that $\mathbf{K}=\mathbf{G}_n+\mathbf{q}$ with $\mathbf{q}\in 1$ BZ and

$$\begin{aligned}C(\mathbf{q},\omega)&=(2\pi)^{-1}\int_{-\infty}^{+\infty}dt\,e^{i\omega t}\sum_m e^{i\mathbf{q}\cdot\mathbf{R}_m}C(\mathbf{R}_m,t)\\&=C(\mathbf{q}+\mathbf{G}_n,\omega)\ ,\end{aligned} \tag{2.42}$$

$$C(\mathbf{R}_m,t)=\int d\omega\int d^3q\,C(\mathbf{q},\omega)e^{-i(\omega t+\mathbf{q}\cdot\mathbf{R}_m)}\ , \tag{2.43}$$

and where

$$C_{ij}^{(2)}(\mathbf{R}_m-\mathbf{R}_n,t)=\langle u_{m,i}(t)u_{n,j}(0)\rangle_c\ , \tag{2.44}$$

$$C_{ijk}^{(3)}(\mathbf{R}_m-\mathbf{R}_n,t)=\langle u_{m,i}(t)u_{m,j}(t)u_{n,k}(0)\rangle_c\ , \tag{2.45}$$

$$C_{ijkl}^{(4,1)}(\mathbf{R}_m-\mathbf{R}_n,t)=\langle u_{m,i}(t)u_{m,j}(t)u_{n,k}(0)\times u_{n,l}(0)\rangle_c\ , \tag{2.46}$$

$$C_{ijkl}^{(4,2)}(\mathbf{R}_m-\mathbf{R}_n,t)=\langle u_{m,i}(t)u_{m,j}(t)u_{m,k}(t)\times u_{n,l}(0)\rangle_c\ . \tag{2.47}$$

The first term in the square brackets in Eq. (2.41) represents the sum of Bragg peaks, whereas the next five terms are those contributions to the diffuse scattering intensity which are proportional up to the fourth power of the displacement field $\mathbf{u}$. But one should recall that the Debye-Waller factor e^{-2W} already contains contributions from arbitrarily high powers of $\mathbf{u}$ [see Eq. (2.37)].

For a lattice without defects Eq. (2.31) is the starting point for the calculation of the cross section for scattering at phonons[22] (see also Refs. 34 and 35). Since in that case the distribution $P(\{\mathbf{u}_m\})$ of the displacements is almost a Gaussian distribution, the higher-order correlations $C^{(n)}$, $n\geq 3$, are very small and can be neglected. However, if the displacements are induced by defects, $P(\{\mathbf{u}_m\})$ is far from being Gaussian[14] so that the higher-order correlations are relevant for the scattering cross section. This becomes obvious already by considering

Eq. (2.33). For that purpose let us decompose $\mathbf{u}_m$ into a phonon contribution $\mathbf{s}_m$ and a defect-induced displacement $\mathbf{w}_m$,

$$\mathbf{u}_m(t)=\mathbf{s}_m(t)+\mathbf{w}_m(t) , \tag{2.48}$$

so that $\mathbf{u}_m(t)=\mathbf{s}_m(t)$ for $\tau_a=0$, $a=1,\ldots,N_H$. Even in the presence of anharmonicities $P(\{\mathbf{s}_m\})=P(\{-\mathbf{s}_m\})$ and consequently

$$\langle[\mathbf{K}\cdot\mathbf{s}_m(t)]^2[\mathbf{K}\cdot\mathbf{s}_n(0)]\rangle_c=0 .$$

On the other hand $P(\{\mathbf{w}_m\})\neq P(\{-\mathbf{w}_m\})$ and therewith

$$\langle[\mathbf{K}\cdot\mathbf{w}_m(t)]^2[\mathbf{K}\cdot\mathbf{w}_n(0)]\rangle_c\neq 0$$

[cf. Eqs. (2.62) and (B6)]. This can be understood by noting that there is no defect configuration $\{\tau_a\}$ which can induce, with equal probability, a displacement field $\mathbf{w}_m\{\tau_a\}$ being the reversed of the displacement field of a single defect $\mathbf{T}^{(1)}=-\mathbf{w}$. Thus

$$\langle[\mathbf{K}\cdot\mathbf{w}_m(t)]^2[\mathbf{K}\cdot\mathbf{w}_n(0)]\rangle_c\neq 0$$

underscores the importance of higher correlation functions for interpreting the scattering cross section of a sample with interstitial defects.

In the conventional derivation of the distortion-induced diffuse scattering intensity thermal vibrations are neglected from the outset. According to Eq. (2.48), however, Eq. (2.41) still contains contributions from both lattice vibrations and defect-induced displacements. The separation between them is discussed most easily in terms of the frequency spectrum. At a fixed reduced wave vector $\mathbf{q}=\mathbf{K}-\mathbf{G}_n$ the structure factor is expected to exhibit two peaks at $\omega=\pm\omega(\mathbf{q})$, which stem from the phonon spectrum of the host lattice, and a quasielastically broadened line at $\omega=0$ (see Fig. 1), which is due to the response of the host lattice to the diffusive motion of the defects.[36,37] As long as these three peaks are well separated one has [see Eq. (2.48)]

$$\langle[\mathbf{K}\cdot\mathbf{u}_m(t)][\mathbf{K}\cdot\mathbf{u}_n(0)]\rangle\cong\langle[\mathbf{K}\cdot\mathbf{w}_m(t)][\mathbf{K}\cdot\mathbf{w}_n(0)]\rangle + \langle[\mathbf{K}\cdot\mathbf{s}_m(t)][\mathbf{K}\cdot\mathbf{s}_n(0)]\rangle , \tag{2.49}$$

i.e., the distribution function $P(\{\mathbf{u}_m\})$ approximately factorizes into one for the static defect-induced displacements $\{\mathbf{w}_m\}$ and one for the thermal vibrations $\{\mathbf{s}_m\}$.

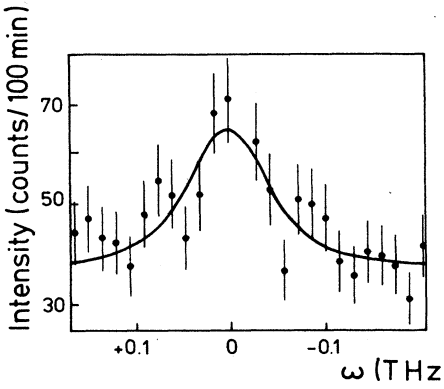

FIG. 1. Energy-resolved diffuse scattering intensity from a $NbD_{0.1}$ single crystal at the wave vector $\mathbf{K}\approx(1.25,1.25,0)(2\pi/a)$. The solid line is a Lorentzian of width 0.082 THz convoluted with the resolution function (Gaussian width 0.05 THz) [with kind permission from E. Burkel *et al.* (Ref. 37)]. The phonon peaks occur at significantly higher frequencies so that in this figure they are out of scale.

In the hydrodynamic limit ($q\to 0$) the width of the quasielastic peak vanishes $\sim Dq^2$, whereby D is the diffusion coefficient of the interstitials. The peak position of the acoustic phonons, however, vanishes $\sim vq$; v is the sound velocity. Thus for small q values the three peaks remain well separated and Eq. (2.49) is valid. For larger q values ($q\approx v/D$) the relaxation and hopping processes are strongly coupled.[38,39] At room temperature typical values of D for hydrogen dissolved in metals is 10^{-5}–10^{-6} cm^2/s.[40] Since $v\approx 10^5$–4×10^5 cm/s, in these cases Eq. (2.49) is valid throughout the Brillouin zone. Only for substantially larger values of D, as they occur at higher temperatures, the three peaks start to overlap.

However, even if these peaks are well separated and Eq. (2.49) is valid, the diffuse scattering intensity is *not* simply the *sum* of two contributions, one being due to the lattice vibrations and the other stemming from static lattice distortions. With $\{\mathbf{w}_m\}$ and $\{\mathbf{s}_m\}$ statistically independent, one has

$$\langle e^{i\mathbf{K}\cdot[\mathbf{u}_m(t)-\mathbf{u}_n(0)]}\rangle\cong\langle e^{i\mathbf{K}\cdot[\mathbf{w}_m(t)-\mathbf{w}_n(0)]}\rangle\langle e^{i\mathbf{K}\cdot[\mathbf{s}_m(t)-\mathbf{s}_n(0)]}\rangle = e^{-2L(\mathbf{K})-2M(\mathbf{K})}\exp\{\langle[\mathbf{K}\cdot\mathbf{w}_m(t)][\mathbf{K}\cdot\mathbf{w}_n(0)]\rangle_c+\cdots\}\exp\{\langle[\mathbf{K}\cdot\mathbf{s}_m(t)][\mathbf{K}\cdot\mathbf{s}_n(0)]\rangle_c+\cdots\} , \tag{2.50}$$

where

$$L(\mathbf{K})=-\ln\langle e^{i\mathbf{K}\cdot\mathbf{w}_m}\rangle$$

and

$$M(\mathbf{K})=-\ln\langle e^{i\mathbf{K}\cdot\mathbf{s}_m}\rangle$$

are the static and thermal Debye-Waller factors, respectively, so that $W(\mathbf{K})=L(\mathbf{K})+M(\mathbf{K})$. By expanding the last two exponential functions in Eq. (2.50) and inserting Eq. (2.50) into Eq. (2.15) one finds that each term of the curly bracket in Eq. (2.41), which contains even correlation functions $C^{(n)}$, consists itself again of two terms. The first one corresponds to the correlations of the static displacements, like $\langle w_{m,i}(t)w_{n,j}(0)\rangle$, and the second one corresponds to the correlations of the thermal displacements, like $\langle s_{m,i}(t)s_{n,j}(0)\rangle$. These latter terms can be

subtracted by using the scattering data of the same, but unloaded sample (see Sec. IV). But according to Eq. (2.50) the square brackets in Eq. (2.41) contain additional terms consisting of *products* of static and thermal correlation functions, like

$$\langle[\mathbf{K}\cdot\mathbf{w}_m(t)][\mathbf{K}\cdot\mathbf{w}_n(0)]\rangle\langle[\mathbf{K}\cdot\mathbf{s}_m(t)][\mathbf{K}\cdot\mathbf{s}_n(0)]\rangle ,$$

etc. The leading term of this sort decays $\sim|\mathbf{R}_m-\mathbf{R}_n|^{-2}$ and leads to a q^{-1} divergence, which is subdominant to the contribution $C^{(2)}_{\text{static}}$ but comparable with $(C^{(2)}_{\text{static}})^2$. In the following we consider therefore in this section without further notice only the correlations of the defect-induced displacements $\{\mathbf{w}_m\}$.

Nonetheless one should be aware of the fact that Eq. (2.50) is only approximately correct, because in a real crystal the interstitials change the force constants of the host lattice and therewith its thermal vibrations. To a certain extent this effect can be taken into account by using for M the phonon spectrum of the loaded host lattice.

In a rigorous approach the displacement correlation functions [Eqs. (2.44)–(2.47)] are calculated from a microscopic Hamiltonian which includes the coupling between the degrees of freedom of the defects and the host lattice.[41] Only in the limiting case where the jump time of the defect between different positions is much smaller than the residence time at a certain position one can introduce occupation numbers $\{\tau_a\}$. Now we specify the relation between the displacements $\{\mathbf{w}_n\}$ and the occupation numbers $\{\tau_a\}$. In order to proceed we use the expansion[14]

$$\mathbf{w}_n(t)=\sum_a \mathbf{T}^{(1)}_{na}[\tau_a(t)-\langle\tau_a\rangle] + \tfrac{1}{2}\sum_{a,b}\mathbf{T}^{(2)}_{nab}[\tau_a(t)\tau_b(t) - \langle\tau_a(t)\tau_b(t)\rangle]+\cdots , \quad (2.51)$$

with $\mathbf{T}^{(1)}_{na}$ as the displacement field of a single defect and $\mathbf{T}^{(2)}_{nab}$ as a contribution to the deviation from their linear superposition; $\mathbf{T}^{(2)}_{naa}=0$.

As long as the motion of the defects is much slower than the thermal vibrations, retardation effects can be taken into account by the replacement

$$\mathbf{T}^{(1)}_{na}\tau_a(t)\rightarrow\int_{-\infty}^{+\infty}dt'\,\mathbf{T}^{(1)}_{na}(t-t')\tau_a(t') ,$$

etc., with $\mathbf{T}^{(1)}_{na}(t)=0$ for $t<0$. $\mathbf{T}^{(1)}_{na}(t-t')dt'$ is the temporal average of the displacement of the lattice site $\mathbf{R}_n$ at time t, if the interstitial site $\mathbf{S}_a$ was occupied from t' until $t'+dt'$, provided dt' is much larger than the inverse phonon frequency. [Recall that, according to Eq. (2.38), $\mathbf{w}_n(t)$ describes the (slow) variation of $\mathbf{u}_m(t)$ as induced by the defects averaged over the (fast) variations due to the phonons described by $\mathbf{s}_m(t)$.]

Equation (2.51) enables us now to analyze systematically each contribution of Eq. (2.41) in terms of the basic correlation functions

$$G^{(n)}=\left\langle\prod_{i=1}^{n}\tau_{a_i}\right\rangle .$$

Due to Eq. (2.32) $C^{(2)}_{ij}(\mathbf{q},\omega)$ is symmetric around the Bragg peak and represents a sum of terms,

$$C^{(2)}_{ij}(\mathbf{q},\omega)=C^{(2,1)}_{ij}(\mathbf{q},\omega)+C^{(2,2)}_{ij}(\mathbf{q},\omega)+\cdots = C^{(2)}_{ij}(-\mathbf{q},\omega) \quad (2.52)$$

with

$$C^{(2,1)}_{ij}(\mathbf{q},\omega)=(2\pi)^2\sum_{\alpha,\beta}\mathbf{T}^{(1)}_{\alpha,i}(\mathbf{q},\omega)\cdot\mathbf{T}^{(1)}_{\beta,j}(-\mathbf{q},-\omega)\cdot G^{(2)}_{\alpha-\beta}(\mathbf{q},\omega) \quad (2.53)$$

and

$$C^{(2,2)}_{ij}(\mathbf{q},\omega)=(2\pi)^3\,\mathrm{Re}\sum_{\alpha,\beta,\gamma}\left[T^{(1)}_{\alpha,i}(\mathbf{q},\omega)\int d^3q'\int d\omega' T^{(2)}_{\beta,\gamma,j}(-\mathbf{q}',-\omega';\mathbf{q}'-\mathbf{q},\omega'-\omega)G^{(3)}_{\alpha-\beta,\alpha-\gamma}(\mathbf{q}',\omega';\mathbf{q}-\mathbf{q}',\omega-\omega')\right] . \quad (2.54)$$

Thus, $C^{(2)}$ is determined by the Fourier transform of the displacement fields of a single defect,

$$\mathbf{T}^{(1)}_{na}=\mathbf{T}^{(1)}(\mathbf{R}_n-\mathbf{S}_a,t-t'),\quad \mathbf{T}^{(2)}_{nab}=\mathbf{T}^{(2)}(\mathbf{R}_n-\mathbf{S}_a,t-t';\mathbf{R}_n-\mathbf{S}_b,t-t'') ,$$

and by the Fourier transform of the correlation functions,

$$\langle\tau_a(t)\tau_b(t')\rangle=G^{(2)}(\mathbf{S}_a-\mathbf{S}_b,t-t'),\quad \langle\tau_a(t)\tau_b(t')\tau_c(t'')\rangle=G^{(3)}(\mathbf{S}_a-\mathbf{S}_b,t-t';\mathbf{S}_a-\mathbf{S}_c,t-t'') ,$$

respectively,

$$\mathbf{T}^{(1)}_{\alpha}(\mathbf{q},\omega)\equiv\mathbf{T}^{(1)}(\mathbf{q},\omega;\mathbf{y}_\alpha) =(2\pi)^{-1}\int_{-\infty}^{+\infty}dt\,e^{i\omega t}\sum_m e^{i\mathbf{q}\cdot\mathbf{R}_m}\mathbf{T}^{(1)}(\mathbf{R}_m-\mathbf{y}_\alpha,t) , \quad (2.55)$$

$$\mathbf{T}^{(2)}_{\alpha,\beta}(\mathbf{q},\omega;\mathbf{q}',\omega')=(2\pi)^{-2}\int_{-\infty}^{+\infty}dt\int_{-\infty}^{+\infty}dt'\,e^{i(\omega t+\omega' t')}\sum_{m,n}e^{i(\mathbf{q}\cdot\mathbf{R}_m+\mathbf{q}'\cdot\mathbf{R}_n)}\mathbf{T}^{(2)}(\mathbf{R}_m-\mathbf{y}_\alpha,t;\mathbf{R}_n-\mathbf{y}_\beta,t') , \quad (2.56)$$

and

$$G^{(2)}_{\alpha-\beta}(\mathbf{q},\omega)=(2\pi)^{-1}\int_{-\infty}^{+\infty}dt\, e^{i\omega t}\sum_m e^{i\mathbf{q}\cdot\mathbf{R}_m}G^{(2)}(\mathbf{R}_m+\mathbf{y}_\alpha-\mathbf{y}_\beta,t)\ , \tag{2.57}$$

$$G^{(3)}_{\alpha-\beta,\alpha-\gamma}(\mathbf{q},\omega;\mathbf{q}',\omega')=(2\pi)^{-2}\int_{-\infty}^{+\infty}dt\int_{-\infty}^{+\infty}dt'\, e^{i(\omega t+\omega' t')}\sum_{m,n} e^{i(\mathbf{q}\cdot\mathbf{R}_m+\mathbf{q}'\cdot\mathbf{R}_n)}G^{(3)}(\mathbf{R}_m+\mathbf{y}_\alpha-\mathbf{y}_\beta,t;\mathbf{R}_n+\mathbf{y}_\alpha-\mathbf{y}_\gamma,t')\ . \tag{2.58}$$

Here we have written the vector of the interstitial site as $\mathbf{S}_a=\mathbf{R}_p+\mathbf{y}_\alpha$ with $\mathbf{R}_p$ being a lattice vector and $\mathbf{y}_\alpha$, $\alpha=1,\ldots,n_H$, describing different interstitial sites within a unit cell. In the derivation of Eqs. (2.53) and (2.54) we used the fact that $\mathbf{T}^{(1)}$ is antisymmetric,

$$\mathbf{T}^{(1)}_\alpha(\mathbf{q})=-\mathbf{T}_{-\alpha}(-\mathbf{q})\ , \tag{2.59}$$

and that $c_\alpha=\langle\tau_a\rangle=c_{-\alpha}$.

Various metal hydrogen systems exhibit a linear increase of the lattice constant as function of the hydrogen concentration up to relatively high values of c.[42] It is not yet clear why the nonlinear effects are so small, but it indicates that for modest values of c, $C^{(2)}$ is dominated by the contribution $C^{(2,1)}$, i.e., by the *two*-point correlation function. In the following we shall adopt this point of view. However, one should keep in mind that, in particular for higher concentrations, even $C^{(2)}$ and therewith the *symmetric* part of the cross section depend on *odd* correlation functions like $G^{(3)}$.

Given the atomic force constants, as they can be inferred from the measured phonon dispersion curves of the host lattice, $\mathbf{T}^{(1)}_\alpha(\mathbf{q},\omega)$ can be calculated.[43,44] Therefore, if one succeeds in extracting $C^{(2)}$ [and therewith $C^{(2,1)}$, see above] from the scattering data (see below), one has direct access to the two-point correlation function $G^{(2)}_{\alpha-\beta}$ [see Eq. (2.53)]. Due to the summation over different interstitial sites within one unit cell $C^{(2,1)}$ cannot be solved explicitly for $G^{(2)}_{\alpha-\beta}$, but with $\mathbf{T}^{(1)}_\alpha$ given for all α one should be able to find a rather unambiguous fit for $G^{(2)}_{\alpha-\beta}$. Moreover, for small values of q both $G^{(2)}_{\alpha-\beta}$ and $\mathbf{T}^{(1)}_\alpha$ become independent from the type of interstitial site so that in the statics, i.e.,

$$C^{(2,2)}(\mathbf{q})=\int d\omega\, C^{(2,1)}(\mathbf{q},\omega),\quad \mathbf{T}^{(1)}(\mathbf{q},\omega)\to\left[\frac{1}{2\pi}\right]\mathbf{T}^{(1)}(\mathbf{q}),\quad \text{and } G^{(2)}(\mathbf{q})=\int d\omega\, G^{(2)}(\mathbf{q},\omega)\ ,$$

Eq. (2.53) reduces to

$$C^{(2,1)}_{ij}(\mathbf{q}\to\mathbf{0})=n_H^2T^{(1)}_i(\mathbf{q})T^{(1)}_j(-\mathbf{q})G^{(2)}(\mathbf{q})\sim q_iq_j/q^4\ , \tag{2.60}$$

where for a defect with cubic symmetry in an elastically isotropic host material

$$\mathbf{T}^{(1)}(\mathbf{q}\to\mathbf{0})=iP[V_{\text{cell}}(c_{12}+2c_{44})]^{-1}\mathbf{q}/q^2\ . \tag{2.61}$$

P denotes the diagonal element of the force dipole tensor $P_{ij}=P\delta_{ij}$, and c_{12} and c_{44} are elastic constants.[44] Thus for small q values $G^{(2)}(\mathbf{q})$ follows unambiguously from $C^{(2,1)}$.

Let us now turn to the term $\propto K^3$ in Eq. (2.41). Again resorting to Eq. (2.51) one obtains with Eq. (2.59)

$$\begin{aligned}C^{(3)}_{ijk}(\mathbf{q},\omega)&=(2\pi)^3\sum_{\alpha,\beta,\gamma}T^{(1)}_{\gamma,k}(-\mathbf{q},-\omega)\int d\omega'\int d^3q'\,T^{(1)}_{\alpha,i}(\mathbf{q}',\omega')T^{(1)}_{\beta,j}(\mathbf{q}-\mathbf{q}',\omega-\omega')G^{(3)}_{\alpha-\beta,\alpha-\gamma}(-\mathbf{q}+\mathbf{q}',-\omega+\omega';\mathbf{q},\omega)\\&=-C^{(3)}_{ijk}(-\mathbf{q},\omega)\ .\end{aligned} \tag{2.62}$$

In Eq. (2.62) we have suppressed higher-order terms involving $\mathbf{T}^{(2)}$, which lead to contributions of four-point correlation functions to $C^{(3)}$. Space does not permit a complete discussion of the terms $\propto K^4$ in Eq. (2.41). Instead we shall evaluate them later within a certain approximation in order to estimate their relevance compared to the terms $\propto K^2$ and $\propto K^3$, respectively (see Appendix B). Nonetheless one finds in general that all three terms $\propto K^4$ are symmetric functions of $\mathbf{q}$ with respect to the center of the 1 BZ [see Eqs. (2.32), (2.34), and (2.35)]. Thus, due to the symmetry of the displacement field of a single defect [Eq. (2.59)], which mediates between the correlations of the interstitials and those of the displacements of the host lattice as seen by the x rays, the cross section separates into two distinct types of contributions: *symmetric* terms, which stem from correlations involving *even* numbers of occupation variables, and *antisymmetric* ones connected with correlations functions of products of occupation numbers with an *odd* number of factors. (As discussed above, the inclusion of $\mathbf{T}^{(2)}$ would modify this statement.) It will be shown below (see Appendix B) that ordinarily the first group of terms is dominated by $G^{(2)}$ and the second one by $G^{(3)}$. Close to the Bragg peak they can be inferred from the symmetric and antisymmetric part of the diffuse scattering intensity around $\mathbf{G}$,

$$\begin{aligned}S_{1,\text{sym}}(\mathbf{G},\mathbf{q},\omega)&=\tfrac{1}{2}[S(\mathbf{G}+\mathbf{q},\omega)+S(\mathbf{G}-\mathbf{q},\omega)]\\&\cong N_L|f_{\text{at}}(\mathbf{G})|^2e^{-2W(\mathbf{G})}\sum_{i,j}G_iG_jC^{(2)}_{ij}(\mathbf{q},\omega)\\&\sim(\mathbf{G}\mathbf{q})^2/q^4,\quad(q\to0)\ ,\end{aligned} \tag{2.63}$$

$$S_{1,\mathrm{asym}}(\mathbf{G},\mathbf{q},\omega)=\tfrac{1}{2}[S_1(\mathbf{G}+\mathbf{q},\omega)-S_1(\mathbf{G}-\mathbf{q},\omega)]$$
$$\cong iN_L|f_{\mathrm{at}}(\mathbf{G})|^2e^{-2W(\mathbf{G})}\sum_{i,j,k}G_iG_jG_kC^{(3)}_{ijk}(\mathbf{q},\omega)$$
$$\sim(\mathbf{Gq})/q^2,\quad (q\to 0)\ . \tag{2.64}$$

Closer to the zone boundary one has to be more careful in order to extract $C^{(2)}$ and $C^{(3)}$ from the scattering data. The first step consists in measuring the intensity of the Bragg peaks in the loaded and unloaded sample. This yields the Debye-Waller factor $e^{-2W(\mathbf{G})}$, whose static part is given by a weighted integral of the two-point correlation function $G^{(2)}$ [see Eqs. (2.37), (2.48), and (2.50)],

$$M(\mathbf{G})=\tfrac{1}{2}(2\pi)^2\sum_{i,j}G_iG_j\int d\omega\int d^3q\sum_i T^{(1)}_{\alpha,i}(\mathbf{q},\omega)T^{(1)}_{\beta,j}(-\mathbf{q},-\omega)G^{(2)}_{\alpha-\beta}(\mathbf{q},\omega)\ . \tag{2.65}$$

Higher-order terms in Eq. (2.65) have been suppressed. Thus, in the second step, with the atomic form factor known, the experimental data allow one to construct the functions

$$S_{\pm}(\mathbf{G},\mathbf{q},\omega)=(2N_L)^{-1}[S_1(\mathbf{G}+\mathbf{q},\omega)|f_{\mathrm{at}}(\mathbf{G}+\mathbf{q})|^{-2}e^{2W(\mathbf{G}+\mathbf{q})}\pm S_1(\mathbf{G}-\mathbf{q},\omega)|f_{\mathrm{at}}(\mathbf{G}-\mathbf{q})|^{-2}e^{2W(\mathbf{G}-\mathbf{q})}]\ . \tag{2.66}$$

With the first two leading terms one obtains

$$S_+(\mathbf{G},\mathbf{q},\omega)=\sum_{i,j}(G_iG_j+q_iq_j)C^{(2)}_{ij}(\mathbf{q},\omega)+i\sum_{i,j,k}(q_iG_jG_k+q_jG_iG_k+q_kG_iG_j+q_iq_jq_k)C^{(3)}_{ijk}(\mathbf{q},\omega) \tag{2.67}$$

and

$$S_-(\mathbf{G},\mathbf{q},\omega)=i\sum_{i,j,k}(G_iG_jG_k+q_iq_jG_k+q_iq_kG_j+q_jq_kG_i)C^{(3)}_{ijk}(\mathbf{q},\omega)+\sum_{i,j}(q_iG_j+q_jG_i)C^{(2)}_{ij}(\mathbf{q},\omega)\ . \tag{2.68}$$

Compared with Eqs. (2.63) and (2.64), $S_\pm$ takes into account correction terms $\sim q/G$, which arise from the momentum prefactors of the contributions $\propto C^{(2)}$ and $\propto C^{(3)}$, respectively, in Eq. (2.41). Although in general $C^{(2)}$ and $C^{(3)}$ cannot be read off from the scattering data as easily as in the case $q\to 0$ [Eqs. (2.63) and (2.64)], they can be reconstructed from the system of equations (2.67) and (2.68), which can be studied for various different vectors $\mathbf{G}_n$.

Note that for a given momentum transfer $\mathbf{K}$, S_+ and S_- determine only the longitudinal parts of $C^{(2)}_{ij}$ and $C^{(3)}_{ijk}$. However, this is sufficient for constructing $G^{(2)}$ and $G^{(3)}$ [Eqs. (2.53) and (2.62)]. Nevertheless all matrix elements of $C^{(2)}_{ij}$ and $C^{(3)}_{ijk}$ can be found by measuring at different reciprocal lattice vectors G and by exploiting symmetry properties.

In sum we have outlined the method of extracting the displacement correlation functions $C^{(2)}$ and $C^{(3)}$ from the symmetric and antisymmetric contributions to the scattering data. Equations (2.52) and (2.53) show that the pair correlation function $\langle\tau_a\tau_b\rangle$ of the interstitial defects can be determined completely from $C^{(2)}$. The results can be checked with the static Debye-Waller factor [Eq. (2.65)].

Since the scattered intensity is a unique function of a single momentum transfer, one cannot expect to explore with a scattering experiment the full three-point correlation $G^{(3)}(\mathbf{q},\mathbf{q}')$, which depends on two momenta. Nonetheless Eq. (2.62) shows that $C^{(3)}$ yields rather detailed information about $\langle\tau_a\tau_b\tau_c\rangle$, namely, for each $\mathbf{q}'$ the weighted integral of $G^{(3)}(\mathbf{q},\mathbf{q}')$ along the lines $\mathbf{q}-\mathbf{q}'$ in the domain of definition of $G^{(3)}$. Thus one is left with basically two options. The first one consists of resorting to theoretical predictions for $G^{(3)}$ and of checking its consistency with $C^{(3)}$. Since the theoretical calculation of $G^{(3)}$ is a very demanding task of current interest even for simple, real liquids (see, e.g., Refs. 45 and 46), for the present system one might turn to the following second option.

If $\mathbf{S}_a$, $\mathbf{S}_b$, and $\mathbf{S}_c$ are well separated, $\langle\tau_a\tau_b\tau_c\rangle$ is expected to factorize into the product of pair correlation functions (Kirkwood superposition approximation[47])

$$\langle\tau_a\tau_b\tau_c\rangle\cong(c_\alpha c_\beta c_\gamma)^{-1}\langle\tau_a\tau_b\rangle\langle\tau_a\tau_c\rangle\langle\tau_b\tau_c\rangle\ . \tag{2.69}$$

Equation (2.69) fails if two or even three sites coincide. However, due to the fact that each site can be occupied only by one interstitial atom one has $\tau_a^n=\tau_a$ for $n=1,2,\ldots$. Thus, just in those cases, in which Eq. (2.69) fails explicitly, $\langle\tau_a\tau_b\tau_c\rangle$ can be expressed exactly in terms of two- and one-point correlation functions. Therefore we suggest the following *modified Kirkwood superposition approximation*:

$$\langle\tau_a\tau_b\tau_c\rangle\cong(c_\alpha c_\beta c_\gamma)^{-1}\langle\tau_a\tau_b\rangle\langle\tau_a\tau_c\rangle\langle\tau_b\tau_c\rangle+[\langle\tau_a\tau_c\rangle-(c_\alpha c_\gamma)^{-1}\langle\tau_a\tau_c\rangle^2]\delta_{a,b}$$
$$+[\langle\tau_a\tau_b\rangle-(c_\alpha c_\beta)^{-1}\langle\tau_a\tau_b\rangle^2](\delta_{a,c}+\delta_{b,c})+2(1-c_\alpha)\delta_{a,b}\delta_{bc,}\ . \tag{2.70}$$

The approximation in Eq. (2.70) has the merits to be both exact in the case that any two points come close together and to be expected to hold at large distances. In Fourier space we have

$$G^{(3)}_{\alpha-\beta,\alpha-\gamma}(\mathbf{q},\mathbf{q}') \approx \int d^3q_1\, G^{(2)}_{\alpha-\beta}(\mathbf{q}_1) G^{(2)}_{\beta-\gamma}(\mathbf{q}_1+\mathbf{q}) G^{(2)}_{\gamma-\alpha}(\mathbf{q}_1+\mathbf{q}+\mathbf{q}')$$
$$+\delta_{\alpha,\beta}\left[G^{(2)}_{\alpha-\gamma}(\mathbf{q}')-(c_\alpha c_\gamma)^{-1}\int d^3q_1\, G^{(2)}_{\alpha-\gamma}(\mathbf{q}_1) G^{(2)}_{\gamma-\alpha}(\mathbf{q}_1+\mathbf{q}')\right]$$
$$+\delta_{\alpha,\gamma}\left[G^{(2)}_{\alpha-\beta}(\mathbf{q})-(c_\alpha c_\beta)^{-1}\int d^3q_1\, G^{(2)}_{\beta-\alpha}(\mathbf{q}_1) G^{(2)}_{\alpha-\beta}(\mathbf{q}_1+\mathbf{q})\right]$$
$$+\delta_{\beta,\gamma}\left[G^{(2)}_{\alpha-\beta}(\mathbf{q}+\mathbf{q}')-(c_\alpha c_\beta)^{-1}\int d^3q_1\, G^{(2)}_{\beta-\alpha}(\mathbf{q}_1) G^{(2)}_{\alpha-\beta}(\mathbf{q}_1+\mathbf{q}+\mathbf{q}')\right]+2(1-c_\alpha)\delta_{\alpha,\beta}\delta_{\beta,\gamma}\ . \quad (2.71)$$

For suggestions on how to implement the superposition approximation directly in Fourier space instead of in real space as in Eq. (2.70), see Refs. 48 and 49; there one has tried to simplify Eq. (2.71) further in order to avoid convolutions.

Suppose now that $G^{(2)}_{\alpha-\beta}(\mathbf{q})$ has been indeed determined from the experimental data in the way we outlined above. Then by inserting this function into Eq. (2.71) one obtains an approximate prediction for the full three-point correlation function $G^{(3)}_{\alpha-\beta,\alpha-\gamma}(\mathbf{q},\mathbf{q}')$, which in turn according to Eq. (2.62) can be compared with $C^{(3)}_{ijk}(\mathbf{q})$. Since $C^{(3)}_{ijk}(\mathbf{q})$ itself follows from the measured diffuse scattering [Eqs. (2.67) and (2.68)] we conclude that based on experimental data alone the comparison between the symmetric and antisymmetric parts of the scattered intensity around a Bragg peak allows one to test the range of validity of the (modified) Kirkwood superposition approximation.

We would like to emphasize that this offers one of the very rare opportunities in which one has direct experimental access to three particle-correlation functions. Their importance goes well beyond the particular lattice-gas system under consideration here. For example, they may play an important role for the freezing and glass transition of ordinary dense liquids because they signal the onset of orientational order.[50,51] Since the calculation of higher-order correlation functions is very difficult, one is frequently compelled to use approximation schemes like the one in Eqs. (2.70) and (2.71). Therefore it is very valuable to have a testing ground for their validity as described above.

III. LAUE CONTRIBUTION AND CROSS TERM

Section II has been devoted primarily to a detailed discussion of the scattering process at the distorted host lattice, i.e., of $S_1(\mathbf{K},\omega)$ [see Eq. (2.14)]. In the case of x-ray scattering at metal-hydrogen systems S_1 is an excellent approximation for the total structure factor S. However, if the scattering power of the interstitial defects is no longer small—as it is the case, e.g., for neutron scattering at metal-hydrogen systems or for x-ray scattering at interstitials like carbon in iron—the scattering process at the interstitials itself, i.e., $S_2(\mathbf{K},\omega)$, and the cross term $S_3(\mathbf{K},\omega)$, represent important contributions to the total cross section. In the literature S_3 is also called size effect or interference term. Here we discuss S_2 and S_3 along the lines of the preceding section.

A. Laue term

By combining Eqs. (2.16) and (2.40) we obtain after a lengthy calculation the following result for the scattering at the interstitial defects themselves ($\mathbf{S}_a=\mathbf{R}_m+\mathbf{y}_\alpha$, $\mathbf{S}_b=\mathbf{R}_n+\mathbf{y}_\beta$):

$$S_2(\mathbf{K},\omega)=N_L|f_{\rm def}|^2\sum_{\alpha,\beta} e^{i\mathbf{K}\cdot(\mathbf{y}_\alpha-\mathbf{y}_\beta)} e^{-[Q_\alpha(\mathbf{K})+Q_\beta(\mathbf{K})]}\{S_{2,\rm Bragg}(\mathbf{K},\omega)+S_{2,\rm sym}(\mathbf{K},\omega)+S_{2,\rm asym}(\mathbf{K},\omega)+S_{2,\rm TDS}(\mathbf{K},\omega)\}\ . \quad (3.1)$$

Provided that the interstitial defects do not form a superlattice structure *all* δ functions are contained in $S_{2,\rm Bragg}$:

$$S_{2,\rm Bragg}(\mathbf{K},\omega)=C^{(1)}_\alpha(\mathbf{K})C^{(2)}_\beta(\mathbf{K})[(2\pi)^3/V_{\rm cell}]\sum_n \delta(\mathbf{K}-\mathbf{G}_n)\delta(\omega)\ , \quad (3.2)$$

where

$$C^{(1)}_\alpha(\mathbf{K})=\langle \tau_a e^{i\mathbf{K}\cdot\mathbf{w}_a}\rangle\ . \quad (3.3)$$

Before we continue to discuss the other terms in Eq. (3.1) let us note that for a particular configuration of the distorted host lattice the positions of the interstitial sites, which are displaced, too, follow from the requirement of minimum potential energy within a unit cell. Thus we are led to decompose these displacements $\mathbf{v}_a(t)$ of the interstitial sites into thermal vibrations $\mathbf{s}_a(t)$ and defect induced displacements [compare Eq. (2.51)]

$$\mathbf{w}_a(t)=\sum_b \int_{-\infty}^{+\infty} dt'\, \mathbf{T}^{(1)}_{ab}(t-t')[\tau_b(t')-\langle\tau_b\rangle]+\cdots,\quad \mathbf{T}^{(1)}_{aa}=\mathbf{0}\ , \quad (3.4)$$

so that

$$\mathbf{v}^{(t)}_a=\mathbf{s}_a(t)+\mathbf{w}_a(t) \quad (3.5)$$

with $\langle\mathbf{v}_a\rangle=\langle\mathbf{w}_a\rangle=\langle\mathbf{s}_a\rangle=\mathbf{0}$ and therewith $\sum_b \mathbf{T}^{(1)}_{ab}c_\beta=\mathbf{0}$. $\mathbf{s}_a$ describes the thermal motion of the unoccupied interstitial sites in the unloaded sample whereas $\mathbf{w}_a$ gives the corrections of these displacements due to the distortions induced by the defects in the loaded sample. Although Eq. (3.5) is the analog of Eq. (2.48), one has to keep in mind that

$\{a,b,\ldots\}$ refers to interstitial sites whereas $\{m,n,\ldots\}$ corresponds to the sites of the host lattice. Therefore $\mathbf{T}^{(1)}_{ab}$ differs from $\mathbf{T}^{(1)}_{mb}$. But both exhibit the same q^{-1} divergence for $q\to 0$ because they become the same function for large distances. $\mathbf{T}^{(1)}_{ab}$ fulfills the symmetry relation $\mathbf{T}^{(1)}_{\alpha-\beta}(\mathbf{q})=-\mathbf{T}^{(1)}_{\alpha-\beta}(-\mathbf{q})$. Within the approximation of Eqs. (3.4) and (3.5) $\{\mathbf{s}_a\}$ and $\{\mathbf{w}_a\}$ are statistically independent so that all terms in Eq. (3.1) carry the same Debye-Waller factor

$$\langle e^{i\mathbf{K}\mathbf{s}_a}\rangle = e^{-Q_\alpha(\mathbf{K})} . \tag{3.6}$$

Due to the inversion symmetry of $\mathbf{T}^{(1)}$ all correlation functions of τ_a containing odd powers of $(\mathbf{K}\cdot\mathbf{w}_a)$ vanish. Thus $C^{(1)}_\alpha(\mathbf{K})$ is real and

$$C^{(1)}_\alpha(\mathbf{K})=e^{-N_\alpha(\mathbf{K})}[c_\alpha-\tfrac{1}{2}\langle\tau_a(\mathbf{K}\cdot\mathbf{w}_a)^2\rangle_c+\cdots] , \tag{3.7}$$

where

$$e^{-N_\alpha(\mathbf{K})}=\langle e^{i\mathbf{K}\cdot\mathbf{w}_a}\rangle \tag{3.8}$$

is the "static" Debye-Waller factor, which is the analog of $L(\mathbf{K})$ in Eq. (2.50); $Q_\alpha(\mathbf{K})$ corresponds to $M(\mathbf{K})$. According to Eq. (3.7) the δ functions in Eq. (3.2) are not simply proportional to $c_\alpha c_\beta$ because the occupation number τ_a at site $\mathbf{S}_a$ is correlated with its displacement $\mathbf{w}_a$ via the neighboring defects [see Eq. (3.4)]. The first correction term in Eq. (3.7) is given by a three-point correlation function. Without this correction term one has $C^{(1)}_\alpha\propto c_\alpha$, which is a one-point correlation function. Therefore in the following $C^{(1)}_\alpha$ is called a (pseudo-) one-point correlation function.

Let us now continue to discuss the various terms in Eq. (3.1). The diffuse scattering, i.e., the last three terms in the curly braces, can be divided into three contributions: those which are symmetric ($S_{2,\mathrm{sym}}$) and antisymmetric ($S_{2,\mathrm{asym}}$), around a Bragg peak $\mathbf{G}_n\neq\mathbf{0}$, respectively, and the thermal diffuse scattering $S_{2,\mathrm{TDS}}$, which contains correlation functions of $\{\mathbf{s}_a\}$. One finds for the symmetric part

$$\begin{aligned}S_{2,\mathrm{sym}}(\mathbf{K},\omega)=&e^{-[N_\alpha(\mathbf{K})+N_\beta(\mathbf{K})]}G^{(2,c)}_{\alpha-\beta}(\mathbf{q},\omega)\\&+\sum_{j,k}K_jK_k\{C^{(1)}_\alpha(\mathbf{K})C^{(1)}_\beta(\mathbf{K})D^{(2,1)}_{\alpha-\beta,jk}(\mathbf{q},\omega)\\&\quad+[e^{-N_\alpha(\mathbf{K})}C^{(1)}_\beta(\mathbf{K})+e^{-N_\beta(\mathbf{K})}C^{(1)}_\alpha(\mathbf{K})]D^{(3,1)}_{\alpha-\beta,jk}(\mathbf{q},\omega)\\&\quad+e^{-[N_\alpha(\mathbf{K})+N_\beta(\mathbf{K})]}D^{(4)}_{\alpha-\beta,jk}(\mathbf{q},\omega)\}+O(K^4) .\end{aligned} \tag{3.9}$$

$G^{(2,c)}_{\alpha-\beta}(\mathbf{q},\omega)$ is the Fourier transform of $\langle\tau_a(t)\tau_b(0)\rangle_c$. The terms $\propto K^2$ consist of the product of two (pseudo-) one-point correlation functions, i.e., $C^{(1)}_\alpha C^{(1)}_\beta$, and a two-point correlation function

$$D^{(2,1)}_{\alpha-\beta,jk}(\mathbf{R}_m-\mathbf{R}_n,t)=\langle w_{a,j}(t)w_{b,k}(0)\rangle_c=D^{(2,1)}_{\beta-\alpha,kj}(\mathbf{R}_n-\mathbf{R}_m,t) , \tag{3.10}$$

a product of one (pseudo-) one-point correlation function, i.e., $C^{(1)}_\alpha$ or $C^{(1)}_\beta$, and a three-point correlation function

$$\begin{aligned}D^{(3,1)}_{\alpha-\beta,jk}(\mathbf{R}_m-\mathbf{R}_n,t)&=\langle\tau_a(t)w_{a,j}(t)w_{b,k}(0)\rangle_c-\tfrac{1}{2}\langle\tau_a(t)w_{b,j}(0)w_{b,k}(0)\rangle_c\\&=D^{(3,1)}_{\beta-\alpha,kj}(\mathbf{R}_n-\mathbf{R}_m,t) ,\end{aligned} \tag{3.11}$$

and at last of a four-point correlation function

$$\begin{aligned}D^{(4)}_{\alpha-\beta,jk}(\mathbf{R}_m-\mathbf{R}_n,t)=&\langle\tau_a(t)\tau_b(0)\rangle_c\langle w_{a,j}(t)w_{b,k}(0)\rangle_c\\&-\tfrac{1}{2}\langle\tau_a(t)\tau_b(0)[w_{a,j}(t)w_{a,k}(t)-w_{a,j}(t)w_{b,k}(0)-w_{b,j}(0)w_{a,k}(t)+w_{b,j}(0)w_{b,k}(0)]\rangle_c\\&+\langle\tau_a(t)w_{b,j}(0)\rangle_c\langle\tau_b(0)w_{a,k}(t)\rangle_c\\=&D^{(4)}_{\alpha-\beta,kj}(\mathbf{R}_n-\mathbf{R}_m,t) .\end{aligned} \tag{3.12}$$

The antisymmetric part has the form

$$S_{2,\mathrm{asym}}(\mathbf{K},\omega)=i\sum_j K_j\{-[e^{-N_\alpha(\mathbf{K})}C^{(1)}_\beta(\mathbf{K})+e^{-N_\beta(\mathbf{K})}C^{(1)}_\alpha(\mathbf{K})]D^{(2,2)}_{\alpha-\beta,j}(\mathbf{q},\omega)+e^{-[N_\alpha(\mathbf{K})+N_\beta(\mathbf{K})]}D^{(3,2)}_{\alpha-\beta,j}(\mathbf{q},\omega)\}+O(K^3) \tag{3.13}$$

and consists of the product of a (pseudo-) one-point correlation function, i.e., $C^{(1)}_\alpha$ or $C^{(1)}_\beta$, and a two-point correlation function

$$D^{(2,2)}_{\alpha-\beta,j}(\mathbf{R}_m-\mathbf{R}_n,t)=\langle\tau_a(t)w_{b,j}(0)\rangle_c=-D^{(2,2)}_{\beta-\alpha,j}(\mathbf{R}_n-\mathbf{R}_m,t) , \tag{3.14}$$

and of a three-point correlation function

$$D^{(3,2)}_{\alpha-\beta,j}(\mathbf{R}_m-\mathbf{R}_n,t)=\langle\tau_a(t)\tau_b(0)[w_{a,j}(t)-w_{b,j}(0)]\rangle=-D^{(3,2)}_{\beta-\alpha,j}(\mathbf{R}_n-\mathbf{R}_m,t)\ . \tag{3.15}$$

Since $D^{(2,2)}$ and $D^{(3,2)}$ are antisymmetric functions of $\mathbf{R}_m-\mathbf{R}_n$ (after they have been summed over α and β) their Fourier transform is purely imaginary so that $S_{2,\mathrm{asym}}$ is indeed real [Eq. (3.13)].

Note that due to the correlations between the occupation number and the corresponding displacement $C^{(1)}_\alpha \neq c_\alpha e^{-N_\alpha}$, so that *one has no longer a common static Debye-Waller factor.* Instead there are four types of terms: those multiplied by $C^{(1)}_\alpha C^{(1)}_\beta$, $C^{(1)}_\alpha e^{-N_\beta}$, $C^{(1)}_\beta e^{-N_\alpha}$, and $e^{-N_\alpha-N_\beta}$, respectively [see Eqs. (3.9) and (3.13)]. Furthermore $S_2(\mathbf{K},\omega)$ and $S_3(\mathbf{K},\omega)$ (see below) differ in their structure from the one of $S_1(\mathbf{K},\omega)$, whose symmetric and antisymmetric parts contain only even and odd correlation functions, respectively. In S_2 and S_3, however, the symmetric part contains also odd and the antisymmetric part also even correlation functions [see Eqs. (3.9), (3.11), (3.13), and (3.14)].

Before we discuss $S_{2,\mathrm{sym}}$ and $S_{2,\mathrm{asym}}$ in more detail, let us finish the description of the various terms in Eq. (3.1). $S_{2,\mathrm{TDS}}$ collects all those contributions, which stem from correlation functions of the thermal vibrations $\{\mathbf{s}_a\}$ and which are not yet absorbed in the thermal Debye-Waller factors. The most important contributions are given by

$$S_{2,\mathrm{TDS}}(\mathbf{K},\omega)=\sum_{j,k}K_jK_k[C^{(1)}_\alpha(\mathbf{K})C^{(1)}_\beta(\mathbf{K})D^{(2,th,1)}_{\alpha-\beta,jk}(\mathbf{q},\omega)+e^{-[N_\alpha(\mathbf{K})+N_\beta(\mathbf{K})]}D^{(2,th,2)}_{\alpha-\beta,jk}(\mathbf{q},\omega)]+O(K^3)\ , \tag{3.16}$$

where

$$D^{(2,th,1)}_{\alpha-\beta,jk}(\mathbf{R}_m-\mathbf{R}_n,t)=\langle s_{a,j}(t)s_{b,k}(0)\rangle=D^{(2,th,1)}_{\beta-\alpha,kj}(\mathbf{R}_n-\mathbf{R}_m,t) \tag{3.17}$$

and

$$D^{(2,th,2)}_{\alpha-\beta,jk}(\mathbf{R}_m-\mathbf{R}_n,t)=\langle\tau_a(t)\tau_b(0)\rangle_c\langle s_{a,j}(t)s_{b,k}(0)\rangle_c=D^{(2,th,2)}_{\beta-\alpha,kj}(\mathbf{R}_n-\mathbf{R}_m,t)\ , \tag{3.18}$$

whose Fourier transforms are symmetric around $\mathbf{q}=\mathbf{0}$.

According to Eq. (3.18) $D^{(2,th,2)}$ is the product of two-point correlation functions. Consider now its first factor $G^{(2)}$. If the occupation numbers are coupled via short-ranged effective interactions, $G^{(2)}$ decays exponentially for $r=|\mathbf{S}_a-\mathbf{S}_b|\to\infty$. If, however, these interactions decay like a power law $\sim r^{-\kappa}$, $G^{(2)}$ cannot vanish more rapidly than $\sim r^{-\kappa}$, too. In metal-hydrogen systems the interactions exhibit oscillations for $r\to\infty$, whose envelope decays $\sim r^{-3}$.[52] Consequently, in these cases $G^{(2)}(\mathbf{q})$ remains finite for $q\to 0$, which is in accordance with the experimental results presented in Sec. IV. *A fortiori* the Fourier transform of $[G^{(2)}\langle\mathbf{s}_a\mathbf{s}_b\rangle_c]$ remains finite for $q\to 0$. This is also true for the integral over ω of the second term in Eq. (3.16) so that $\int d\omega\, S_{2,\mathrm{TDS}}(\mathbf{K},\omega)\sim c_\alpha c_\beta(K/q)^2$ for $q\to 0$. [The terms $O(K^2)$ contain contributions $\sim q^{-1}$.]

Because $S_{2,\mathrm{TDS}}$ vanishes for the unloaded sample, it cannot be subtracted by using the scattering data of the host lattice without defects. However, the *inelastic* scattering data allow one to identify the contributions of TDS due to their characteristic $\mathbf{q}$ and ω dependence, so that $S_{2,\mathrm{TDS}}$ can indeed be subtracted.[53] The elimination of terms like $D^{(2,th,2)}$ is less obvious. Although they are subdominant near the center of the BZ, their importance further away from $\mathbf{q}=\mathbf{0}$ remains to be checked. Likewise this applies also to S_1 and S_3.

After this subtraction procedure the energy integrated structure factor $S_2(\mathbf{q})$ is given by $S_{2,\mathrm{sym}}+S_{2,\mathrm{asym}}$. It is interesting to compare these contributions with the corresponding ones in S_1. Whereas in S_1 each term, which contains correlations of n factors τ, is multiplied by n factors $\mathbf{T}^{(1)}_{ma}$ of the displacement field, too, in S_2 only $(n-2)$ factors $\mathbf{T}^{(1)}_{ab}$ enter. As a consequence the symmetric part $S_{2,\mathrm{sym}}$ ($\mathbf{G}_n\neq\mathbf{0},\mathbf{q}$) is dominated by the *de facto* four-point correlation functions ($\propto K^2$) which lead to a q^{-2} divergence, whereas the lowest contribution $G^{(2,c)}$ remains finite for $q\to 0$ [see Eq. (3.9)]. This q^{-2} divergence is caused by $D^{(2,1)}$, which we regard as a *de facto* four-point correlation function because it is multiplied by two (pseudo-) one-point correlation functions [Eqs. (3.9) and (3.10)],

$$\begin{aligned}D^{(2,1)}_{\alpha-\beta,jk}(\mathbf{q})&=\sum_{\gamma,\delta}T_{\alpha-\gamma,j}(\mathbf{q})T_{\beta-\delta,k}(-\mathbf{q})G^{(2,c)}_{\gamma-\delta}(\mathbf{q})\\&\sim q^{-2}G^{(2)}(\mathbf{q}=\mathbf{0})\quad\text{for } q\to 0\ .\end{aligned} \tag{3.19}$$

Here $G^{(2,c)}(\mathbf{q})$ enters in a similar way as into S_1 [compare Eq. (2.53)]. The behavior of the other terms $\propto K^2$ is more complicated. Within the approximation of Appendix A the first term in Eq. (3.11) vanishes so that due to the second one

$$\begin{aligned}D^{(3,1)}_{\alpha-\beta,jk}(\mathbf{R}_m-\mathbf{R}_n,0)&\cong-\tfrac{1}{2}c_\alpha(1-c_\alpha)(1-2c_\alpha)[T^{(1)}_{\alpha-\beta,j}(\mathbf{R}_m-\mathbf{R}_n)T^{(1)}_{\alpha-\beta,k}(\mathbf{R}_m-\mathbf{R}_n)]\\&\sim|\mathbf{R}_m-\mathbf{R}_n|^{-4}\end{aligned} \tag{3.20}$$

and therewith

$$\lim_{\mathbf{q}\to\mathbf{0}}D^{(3,1)}_{\alpha-\beta,jk}(\mathbf{q})<\infty\ . \tag{3.21}$$

The first term in Eq. (3.12) decays sufficiently fast due to the factor $\langle\tau_a\tau_b\rangle_c$ (see above), the second one vanishes within

the approximation of Appendix A so that due to the third term

$$D^{(4)}_{\alpha-\beta,jk}(\mathbf{R}_n-\mathbf{R}_m,0)\cong -c_\alpha c_\beta(1-c_\alpha)(1-c_\beta)[T^{(1)}_{\alpha-\beta,j}(\mathbf{R}_m-\mathbf{R}_n)T^{(1)}_{\alpha-\beta,k}(\mathbf{R}_m-\mathbf{R}_n)]$$
$$\sim|\mathbf{R}_m-\mathbf{R}_n|^{-4} \tag{3.22}$$

and therewith

$$\lim_{\mathbf{q}\to 0} D^{(4)}_{\alpha-\beta,jk}(\mathbf{q})<\infty\ . \tag{3.23}$$

Therefore we conclude that for $\mathbf{G}_n\neq\mathbf{0}$ and $\mathbf{q}\to\mathbf{0}$ the symmetric part of S_2 is dominated by

$$S_{2,\mathrm{sym}}(\mathbf{G}_n\neq\mathbf{0},\mathbf{q}\to\mathbf{0})\cong C^{(1)}_\alpha(\mathbf{G}_n)C^{(1)}_\beta(\mathbf{G}_n)\sum_{\gamma,\delta}[\mathbf{G}_n\cdot\mathbf{T}^{(1)}_{\alpha-\gamma}(\mathbf{q})][\mathbf{G}_n\cdot\mathbf{T}^{(1)}_{\beta-\delta}(\mathbf{q})]G^{(2,c)}_{\gamma-\delta}(\mathbf{q})$$
$$\sim q^{-2}\ . \tag{3.24}$$

In particular for larger values of q the importance of those terms which happen to vanish within the crude approximation of Appendix A remains to be checked.

Let us now turn to the antisymmetric part of S_2 [Eq. (3.13)]. Again within the approximation of Appendix A the true three-point correlation function $D^{(3,2)}$ vanishes [Eq. (3.15)]. Thus to leading order the antisymmetric part of S_2 is dominated by

$$S_{2,\mathrm{asym}}(\mathbf{G}_n\neq\mathbf{0},\mathbf{q}\to\mathbf{0})\cong -i[e^{-N_\alpha(K)}C^{(1)}_\beta(\mathbf{K})+e^{-N_\beta(K)}C^{(1)}_\alpha(\mathbf{K})]\sum_\gamma[\mathbf{K}\cdot\mathbf{T}^{(1)}_{\beta-\gamma}(-\mathbf{q})]G^{(2,c)}_{\alpha-\gamma}(\mathbf{q})$$
$$\sim q^{-1}\ . \tag{3.25}$$

Thus we conclude that for $\mathbf{G}_n\neq\mathbf{0}$ and $\mathbf{q}\to\mathbf{0}$ the symmetric part of S_2 diverges $\sim q^{-2}$ and the antisymmetric part $\sim q^{-1}$. This is the same behavior as of S_1. However, in contrast to S_1, here both the symmetric and the antisymmetric part are to leading order determined by the two-point correlation function $G^{(2,c)}$. Roughly speaking in $S_{2,\mathrm{sym}}$ $G^{(2,c)}$ is multiplied by c^2T^2, whereas in $S_{2,\mathrm{asym}}$ it is multiplied by cT.

The divergence of $S_{2,\mathrm{sym}}$ masks the direct observation of $G^{(2,c)}$ [see the first term in Eq. (3.9)]. If one insists on this direct observation, one is forced to perform small angle scattering around $\mathbf{G}=\mathbf{0}$.[54] In this case $\mathbf{K}=\mathbf{q}$ and *all* terms in Eq. (3.1), as well as in S_1 and S_3, become symmetric around $\mathbf{q}=\mathbf{0}$. Furthermore *all* divergences for $\mathbf{q}\to\mathbf{0}$ disappear. If the thermal diffuse scattering has been subtracted as described above, the first term in Eq. (3.9) has to compete only with the (now finite) displacement-induced contributions in S_1, S_2, and S_3. To leading order these contributions contain one factor T of the displacement field [see Eq. (3.25)]. If the displacements are small, i.e., if their strength A [Eq. (B2)] is small, the first term in Eq. (3.9) dominates S_1, S_2, and S_3. Under these circumstances the total structure factor S can be identified directly with the structure factor $G^{(2,c)}$ of the interstitial defects.[54] The question, whether this procedure is reliable even for larger values of q, remains to be checked numerically for each system under consideration. Furthermore one has to keep in mind that for this direct observation of $G^{(2)}$ it is indispensable to separate the thermal diffuse scattering by inelastic neutron scattering, whereas by using x-ray scattering as described in Sec. II the TDS can be eliminated by comparing the data with those of the unloaded sample. In addition within certain limits this latter approach is not limited to small displacement fields.

B. Cross term

In the second half of this section we now discuss the structure of the cross term $S_3(\mathbf{K},\omega)$. In analogy to S_1 and S_2 one obtains from Eqs. (2.17) and (2.39)

$$S_3(\mathbf{K},\omega)=2N_L\,\mathrm{Re}\left\{f_{\mathrm{at}}f^*_{\mathrm{def}}\,e^{-[L(\mathbf{K})+M(\mathbf{K})]}\sum_\alpha e^{-i\mathbf{K}\cdot\mathbf{y}_\alpha-Q_\alpha(\mathbf{K})}\right.$$
$$\left.\times[S_{3,\mathrm{Bragg}}(\mathbf{K},\omega)+S_{3,\mathrm{sym}}(\mathbf{K},\omega)+S_{3,\mathrm{asym}}(\mathbf{K},\omega)+S_{3,\mathrm{TDS}}(\mathbf{K},\omega)]\right\}\ . \tag{3.26}$$

In the absence of a superlattice structure of the interstitials $S_{3,\mathrm{Bragg}}$ contains all δ functions,

$$S_{3,\mathrm{Bragg}}(\mathbf{K},\omega)=C^{(1)}_\alpha(\mathbf{K})[(2\pi)^3/V_{\mathrm{cell}}]\sum_n\delta(\mathbf{K}-\mathbf{G}_n)\delta(\omega)\ . \tag{3.27}$$

The other terms in the curly bracket of Eq. (3.26) represent the contribution to the diffuse scattering. The symmetric part of the distortion-induced term is given by (here $\mathbf{S}_a=\mathbf{R}_n+\mathbf{y}_\alpha$)

$$S_{3,\mathrm{sym}}(\mathbf{K},\omega)=\sum_{j,k}K_jK_k[(2\pi)^2C^{(1)}_\alpha(\mathbf{K})\sum_{\beta,\gamma}T^{(1)}_{\alpha-\beta,j}(\mathbf{q},\omega)T^{(1)}_{\gamma,k}(-\mathbf{q},-\omega)G^{(2,c)}_{\beta-\gamma}(\mathbf{q},\omega)+e^{-N_\alpha(\mathbf{K})}E^{(3,1)}_{\alpha,jk}(\mathbf{q},\omega)]+O(K^4)\ , \tag{3.28}$$

where

$$E^{(3,1)}_{\alpha,jk}(\mathbf{R}_n-\mathbf{R}_m,t)=\langle\tau_a(0)w_{a,j}(0)w_m(t)\rangle_c-\tfrac{1}{2}\langle\tau_a(0)w_{m,j}(t)w_{m,k}(0)\rangle_c$$
$$=E^{(3,1)}_{\alpha,kj}(\mathbf{R}_m-\mathbf{R}_n,t)\ . \tag{3.29}$$

Note that $\mathbf{T}^{(1)}_{\alpha-\beta}(\mathbf{q},\omega)$ is the Fourier transform of $\mathbf{T}^{(1)}_{ab}(t-t')$, which must be distinguished from $\mathbf{T}^{(1)}_{mc}(t-t')$ whose Fourier transform is denoted by $\mathbf{T}^{(1)}_{\gamma}(\mathbf{q},\omega)$.

For the antisymmetric contribution of $S_3(\mathbf{K},\omega)$ one obtains

$$S_{3,\mathrm{asym}}(\mathbf{K},\omega)=ie^{-N_\alpha(\mathbf{K})}\sum_j K_j\sum_\beta 2\pi T^{(1)}_{\beta,j}(\mathbf{q},\omega)G^{(2,c)}_{\alpha-\beta}(\mathbf{q},\omega)$$
$$+i\sum_{i,j,k}K_iK_jK_k[e^{-N_\alpha(\mathbf{K})}E^{(4)}_{\alpha,ijk}(\mathbf{q},\omega)+C^{(1)}_\alpha E^{(3,2)}_{\alpha,ijk}(\mathbf{q},\omega)]+O(K^5)\ . \tag{3.30}$$

The four-point correlation function $E^{(4)}$ consists of three terms,

$$E^{(4)}_{\alpha,ijk}(\mathbf{R}_n-\mathbf{R}_m,t)=\tfrac{1}{2}\langle\tau_a(0)w_{a,i}(0)w_{m,j}(t)[w_{m,k}(t)-w_{a,k}(0)]\rangle_c$$
$$-\tfrac{1}{6}\langle\tau_a(0)w_{m,i}(t)w_{m,j}(t)w_{m,k}(t)\rangle_c+\langle\tau_a(0)w_{m,i}(t)\rangle_c\langle w_{a,j}(0)w_{m,k}(t)\rangle_c\ , \tag{3.31}$$

which are antisymmetric with respect to $\mathbf{R}_n-\mathbf{R}_m$. Equation (3.30) contains also the product of a (pseudo-) one-point correlation function and a three-point correlation function

$$E^{(3,2)}_{\alpha,ijk}(\mathbf{R}_n-\mathbf{R}_m,t)=\tfrac{1}{2}\langle w_{a,i}(0)w_{m,j}(t)[w_{m,k}(t)-w_{a,k}(0)]\rangle_c\ , \tag{3.32}$$

which is also antisymmetric. Consequently $S_{3,\mathrm{asym}}$ is real.

Finally the leading contribution of S_3 to the thermal diffuse scattering is

$$S_{3,\mathrm{TDS}}(\mathbf{K},\omega)=\sum_{i,j}K_iK_jC^{(1)}_\alpha(\mathbf{K})E^{(2,th,1)}_{\alpha,ij}(\mathbf{q},\omega)+i\sum_{i,j,k}K_iK_jK_ke^{-N_\alpha(\mathbf{K})}E^{(2,th,2)}_{\alpha,ijk}(\mathbf{q},\omega)+O(K^4) \tag{3.33}$$

with

$$E^{(2,th,1)}_{\alpha,ij}(\mathbf{R}_n-\mathbf{R}_m,t)=\langle s_{a,i}(0)s_{m,j}(t)\rangle_c \tag{3.34}$$

and

$$E^{(2,th,2)}_{\alpha,ijk}(\mathbf{R}_n-\mathbf{R}_m,t)=\langle\tau_a(0)w_{m,i}(t)\rangle_c\langle s_{a,j}(0)s_{m,k}(t)\rangle_c\ . \tag{3.35}$$

Equations (3.33) and (3.35) show that the thermal diffuse scattering contains also antisymmetric contributions. As in the case of S_1 and S_2 one has

$$\int d\omega\, S_{3,\mathrm{TDS}}(\mathbf{K},\omega)\sim q^{-2}\quad\text{for } \mathbf{G}_n\neq\mathbf{0}\ \text{ and }\ \mathbf{q}\to\mathbf{0}\ .$$

By applying the approximation of Appendix A one finds that for $\mathbf{q}\to\mathbf{0}$ $E^{(3,1)}$ as well as $E^{(4)}$ and $E^{(3,2)}$ are subdominant compared to the leading terms of $S_{3,\mathrm{sym}}$ and $S_{3,\mathrm{asym}}$, respectively. Within this approximation the first term in Eq. (3.29) vanishes so that

$$E^{(3,1)}_{\alpha,jk}(\mathbf{R}_n-\mathbf{R}_m,0)\cong c_\alpha(1-c_\alpha)(1-2c_\alpha)T^{(1)}_{ma,j}T^{(1)}_{ma,k}\sim|\mathbf{R}_n-\mathbf{R}_m|^{-4}\ , \tag{3.36}$$

and therewith

$$\lim_{\mathbf{q}\to\mathbf{0}}E^{(3,1)}_{\alpha,jk}(\mathbf{q})<\infty\ . \tag{3.37}$$

Again within this approximation the first term in Eq. (3.31) vanishes. For the other two one has

$$E^{(4)}_{\alpha,ijk}(\mathbf{R}_n-\mathbf{R}_m,0)\cong-\tfrac{1}{6}c_\alpha(1-c_\alpha)(1-6c_\alpha+6c_\alpha^2)T^{(1)}_{ma,i}T^{(1)}_{ma,j}T^{(1)}_{ma,k}+c_\alpha(1-c_\alpha)T^{(1)}_{ma,i}\sum_c c_\gamma(1-c_\gamma)T^{(1)}_{ac,j}T^{(1)}_{mc,k}$$
$$\sim|\mathbf{R}_n-\mathbf{R}_m|^{-3}\ . \tag{3.38}$$

The first term in Eq. (3.38) decays $\sim|\mathbf{R}_n-\mathbf{R}_m|^{-6}$ and leads to a finite value for $\mathbf{q}\to\mathbf{0}$, whereas the second term gives rise to at most a logarithmic divergence of $E^{(4)}(\mathbf{q}\to\mathbf{0})$. Finally, $E^{(3,2)}$ vanishes within this crude approximation.

Thus we can summarize our results for the interference term by comparing Eq. (3.24) with Eq. (3.28) and Eq. (3.25) with Eq. (3.30). We find that both in S_2 and S_3 the symmetric parts of the diffuse scattering diverge $\sim q^{-2}$ and the antisymmetric parts $\sim q^{-1}$ for $\mathbf{G}_n\neq\mathbf{0}$ and $\mathbf{q}\to\mathbf{0}$. In addition the leading behavior of all four contributions—$S_{2,\mathrm{sym}}$, $S_{2,\mathrm{asym}}$, $S_{3,\mathrm{sym}}$, and $S_{3,\mathrm{asym}}$—are characterized *explicitly* by the Fourier transform of $\langle\tau_a(t)\tau_b(0)\rangle_c$ and by one or two factors of the displacement field $\mathbf{T}^{(1)}$ of a single defect. This has to be contrasted with the term S_1 discussed in Sec. II. In S_1 only the symmetric part $S^{(1)}_{\mathrm{sym}}$ exhibits a similar structure as its counterparts in S_2 and S_3. However, $S_{1,\mathrm{asym}}$ is determined to leading order by a *true* three-point correlation function.

Obviously the interpretation of the total cross section is much easier if the total sum $S=S_1+S_2+S_3$ is dominated by only one of these three terms. There are several situations in which this simplification is indeed fulfilled.

The first one concerns x-ray scattering at metal-hydrogen systems, which has been discussed in detail in Sec. II and for which experimental results will be presented in Sec. IV. In this case S_1 competes with S_3, but $S_3/S_1\propto|f_{me}|^{-1}\approx0.02$. S_2 is irrelevant because $S_2/S_1\propto|f_{me}|^{-2}\approx4\times10^{-4}$.

As a second example consider neutron scattering at the vanadium-deuterium system VD_x. This situation is complementary to the above one, because the coherent scattering length of vanadium is much smaller than that of deuterium so that S_2 is the dominant term. As above the cross term S_3 is the leading correction term with $S_3/S_2\propto|f_V/f_D|\approx0.06$. S_1 is negligible because $S_1/S_2\propto|f_V/f_D|^2\approx3.6\times10^{-3}$. One disadvantage of this system is the strong incoherent neutron scattering and absorption of vanadium.

Thus, we conclude this section by noting that despite its complexity the thorough analysis of the cross section of x-ray or neutron scattering at disordered crystals allows one to have an extraordinarily close look at the liquidlike structural properties of the interstitial particles.

IV. COMPARISON WITH EXPERIMENTAL DATA

In this section we analyze experimental data in order to extract from them those correlation functions of point defects which have been discussed in Secs. II and III. With respect to this aim the existing relevant data in the literature can be divided into five distinct groups.

The first group contains all those experimental investigations of diffuse scattering which interpret their data with the help of structure models including a certain type of disorder. The authors usually did not intend to analyze the aforementioned correlation functions.[55,56]

The second group is concerned with the important application of the correlation factor in Huang diffuse scattering from defect clustering in neutron or electron irradiated crystals[57–60] or in alkali halogenides containing color centers.[18,19] In these systems the defects vanish after annealing at high temperatures so that after a subsequent cooling it is possible to study the same sample but now without defects. The difference of the scattered intensities between these two states of the crystal yields directly the contribution from the defects alone. However, in most cases the correlations in these systems corresponds to nonequilibrium configurations, which can be studied only under restricted conditions, e.g., at low temperatures. Furthermore, under these circumstances it is difficult to obtain reproducible results. Therefore the second group cannot be used to test, e.g., theoretical predictions for correlation functions of defects in thermal equilibrium.

Thus one is led to consider hydrogen in metals, which can be investigated under conditions of thermal equilibrium over a wide range of temperature and concentration. For the metal-hydrogen systems there are basically two possibilities to separate the distortion-induced diffuse scattering from the other contributions.

According to the discussion following Eq. (3.18) the first possibility consists of performing inelastic neutron scattering experiments, which allow one to subtract the characteristic contributions from the thermal diffuse scattering. However, so far this third group of experiments[53] has determined only the $\mathbf{q}\to\mathbf{0}$ limit of the correlation functions. In addition, this subtraction method is restricted to rather favorable conditions.

The second possibility for separating the various diffuse contributions is realized by x-ray scattering experiments at one and the same host crystal by comparing the scattered intensities from the loaded and unloaded sample, respectively. This technique can be exploited in two ways. In the first one, which forms the fourth group of experiments[61,62] having been initiated by Metzger, Peisl, and Wanagel by using hydrogen in niobium,[61] one studies only low-defect concentrations (between 1 and 3 at. % H/Nb). As a consequence the dissolved hydrogen atoms form a dilute lattice gas so that the correlations between the defects resemble closely those of a random distribution as described in Appendix A, $\langle\tau_a\tau_b\rangle_c=c_a\delta_{a,b}$ [Eq. (A6), $c\ll1$] and therewith

$$G^{(2)}_{\alpha-\beta}(\mathbf{q},\omega)\cong c_\alpha\delta(\omega)\delta_{\alpha,\beta}$$

is constant throughout the Brillouin zone [Eq. (2.57)]. Thus according to Eqs. (2.41) and (2.53)

$$S_1(\mathbf{K})\cong\left|\sum_\alpha c_\alpha\mathbf{K}\cdot\mathbf{T}^{(1)}_\alpha(\mathbf{q})\right|^2,$$

which dominates S. Therefore these scattering data allow one to obtain information about the strength and the symmetry of the displacement field $\mathbf{T}^{(1)}_n$, in particular for large distances, i.e., $|\mathbf{R}_n-\mathbf{S}_a|\gg$ lattice constant.[61]

These experiments have been extended to high hydrogen concentrations[62,63] forming the fifth group in our discussion. At this high concentration the interstitials are strongly correlated. Thus by using the reversed approach of the fourth group discussed above, here one can indeed determine the desired nontrivial correlation function

$G^{(2)}_{\alpha-\beta}(\mathbf{q})$. In contrast to the first four groups, these experiments fulfill all our requirements and therefore we discuss their results in some detail.

Actually these experiments at high hydrogen concentrations have been performed by using a $Nb_{1-y}Mo_y$ alloy as a host lattice instead of pure Nb. (Mo, which is the neighbor element of Nb in the periodic system with one electron more, forms a continuous series of solid solutions with Nb, all having the same bcc structure. There is no indication of a phase transition in these alloys.) The use of this alloy allows one to study additionally the influence of randomly distributed Mo atoms on the phase transition of the dissolved hydrogen compared with that in an ideal Nb host lattice. These effects of the Mo atoms, which act like a random field, have been discussed elsewhere[64] and are not the topic of the present paper. Here we use these data in order to demonstrate how to extract from them the correlation functions discussed in Sec. II. Mainly we analyze the scattering data from $Nb_{1-y}Mo_yD_x$ with $y=0.01$. (Deuterium was chosen in order to facilitate eventual neutron scattering experiments at the same sample. In the following we do not distinguish between H and D.) For $y=0.01$ the hydrogen atoms exhibit a phase diagram, which has *the same topology* as a pure NbD_x system with $y=0$, which is shown in Fig. 2. The gaslike (α) and liquidlike (α') phases of the hydrogen lattice gas are phase separated below the phase-transition temperature $T_c(x)$. At low temperatures and high concentrations one finds various solid phases like, e.g., the β phase. Thus this phase diagram resembles closely that of an ordinary liquid. For more details see Ref. 4.

Here we want to make a remark concerning our notation. The mean number of dissolved hydrogen divided by the number of interstitial sites $c_\alpha=\langle\tau_\alpha\rangle$ varies between 0 and 1. At high temperatures the interstitial sites—there are n_H of them per host atom—are equivalent so that $c_\alpha=c$ is independent of α. The hydrogen concentration per host atom is denoted as $x=\sum_\alpha c_\alpha$ and can vary between 0 and n_H. For Nb $n_H=6$, but a strong hard-core repulsion between the hydrogen atoms limits x to a value of about 1 (see Fig. 2).

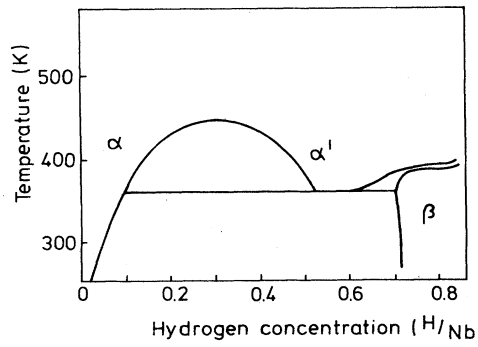

FIG. 2. Phase diagram of hydrogen dissolved in a pure Nb host lattice (Ref. 4). The figure shows the phase boundaries as function of temperature (T) and hydrogen concentration (x). α and α' are the gaslike and liquidlike phases, respectively, which are separated by $T_c(x)$. β is one of the solid phases. Note that in a $Nb_{0.99}Mo_{0.01}$ alloy the phase diagram of the dissolved hydrogen has the same topology but $T_c(x)$ is about 10% lower and slightly distorted (Ref. 65).

The phase diagram of $Nb_{0.99}Mo_{0.01}D_x$ is not yet mapped out completely. However, based on precise measurements at certain selected values of x one knows, that 1 at. % Mo leads to a lowered ($\approx -10\%$) and slightly deformed coexistence line $T_c(x)$.[65] (Note that already 5 at. % Mo wipe out the $\alpha-\alpha'$ transition.[65]) Thus apart from the actual numbers the reader, if necessary, can follow the subsequent discussion by referring to Fig. 2.

Figure 3 displays the raw data of the diffuse scattering around the $G_{(330)}$ Bragg peak from a $Nb_{0.99}Mo_{0.01}$ single crystal (circles) and from the same crystal loaded *in situ* with $x=0.31$ (crosses). Since the diffuse scattering intensity depends on $G=|\mathbf{G}|$ roughly $\sim G^2\exp(-G^2)$ [see Eq. (2.41)], it turns out that around the (330) Bragg peak one obtains the highest intensity. $T=400$ K is chosen such that for $x=0.31$ one is slightly above the maximum of $T_c(x)$, which gives rise to a particularly enhanced diffuse scattering. The angular deviation $\Delta\theta=\theta-\theta_{\text{Bragg}}$ measures the momentum transfer $\mathbf{q}$ parallel to $\mathbf{G}_{(330)}$. As one can see the hydrogen leads to an increase of the diffuse scattering caused by the additional distortion of the host lattice.

In order to proceed one takes the difference between the scattered intensity from the loaded and unloaded sample. Following Eq. (2.63) we form the symmetric part of the diffuse scattering intensity in order to obtain the two-point correlation function without contributions from odd correlation functions. After dividing out the Debye-Waller factor, the atomic form factor and the polarization prefactor, Fig. 4 shows the symmetric part of the diffuse scattering intensity in a double logarithmic plot. As expected asymptotically for $q=|\mathbf{q}|\to 0$ one finds the slope -2, which signals the familiar q^{-2} divergence

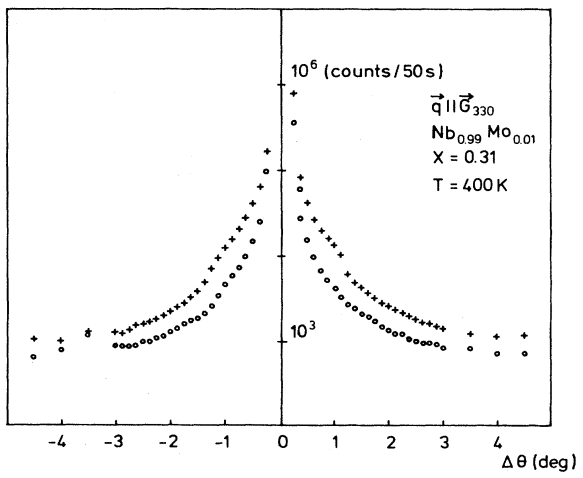

FIG. 3. Raw data of the diffuse scattering intensity (counts per 50 s) around the (330) Bragg peak $\mathbf{G}$ of a $Nb_{0.99}Mo_{0.01}$ alloy loaded with deuterium ($x=0.31$, crosses) and unloaded ($x=0$, circles), respectively, at $T=400$ K. $\Delta\theta$ measures the angular deviation $\theta-\theta_{\text{Bragg}}$ in degree from the Bragg peak position θ_{Bragg} in the direction parallel to $\mathbf{G}_{(330)}$.

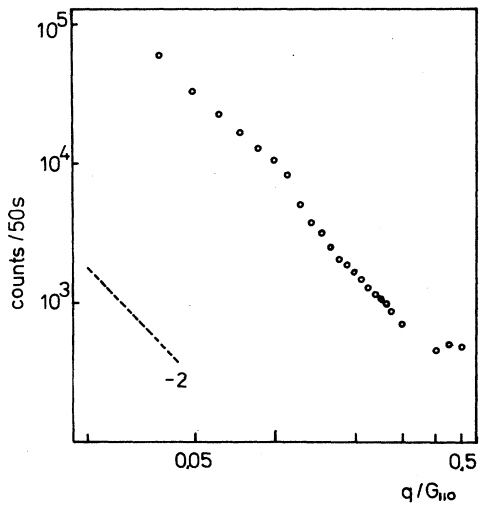

FIG. 4. Double logarithmic plot of the symmetric part of the scattering intensity difference in Fig. 3 without Debye-Waller factor, atomic form factor and polarization factor. The momentum transfer $q=|\mathbf{q}|$ is given in units of $G_{110}=|\mathbf{G}_{(110)}|$. The slope -2 signals the typical q^{-2} divergence for $q\to 0$ in the Huang diffuse scattering.

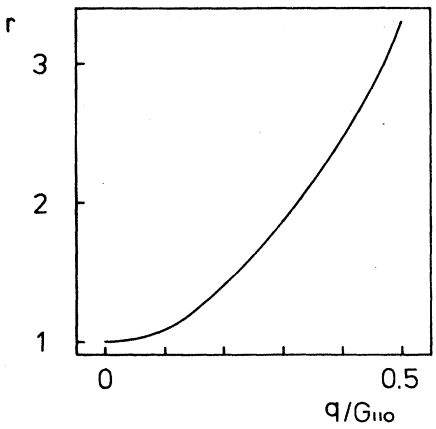

FIG. 5. Ratio r between the correct lattice expression for $[|\mathbf{G}_{(330)}\cdot\mathbf{T}^{(1)}_{\text{latt}}(\mathbf{q})|^2+|\mathbf{q}\cdot\mathbf{T}^{(1)}_{\text{latt}}(\mathbf{q})|^2]$ and its continuum approximation $[|\mathbf{G}_{(330)}\cdot\mathbf{T}^{(1)}_{\text{cont}}(\mathbf{q})|^2+|\mathbf{q}\cdot\mathbf{T}^{(1)}_{\text{cont}}(\mathbf{q})|^2]$ as a function of q/G_{110}. Already for q values at half of the zone boundary the continuum theory overestimates the displacement field seriously.

of the Huang scattering [see Eq. (B4)]. Here it should be noted that one has to apply carefully several correction factors to this difference,[31] especially for the static and dynamic Debye-Waller factors, which were determined separately. The measured intensities were converted to a scattering cross section using an independent measurement of the scattering intensity of an amorphous sample.[8] This is indispensable in order to obtain absolute values of the two-point correlation function (see below).

According to our estimates in Appendix B the symmetric part of the diffuse scattering is dominated by the two-point correlation function. Thus, according to the discussion above we have now extracted from our data [compare Eq. (2.67), $C^{(3)}$ has been neglected, see below] the following expression [see Eq. (2.53)]:

$$\sum_{i,j}(G_iG_j+q_iq_j)C^{(2)}_{ij}(\mathbf{q}) = \sum_{\alpha,\beta}\{[\mathbf{G}\cdot\mathbf{T}^{(1)}_{\alpha}(\mathbf{q})][\mathbf{G}\cdot\mathbf{T}^{(1)}_{\beta}(-\mathbf{q})] +[\mathbf{q}\cdot\mathbf{T}^{(1)}_{\alpha}(\mathbf{q})][\mathbf{q}\cdot\mathbf{T}^{(1)}_{\beta}(-\mathbf{q})]\}G^{(2)}_{\alpha-\beta}(\mathbf{q})\ . \quad (4.1)$$

In order to obtain the Fourier transform of the two-point correlation $G^{(2)}$, one has to determine the Fourier transform of the displacement field $\mathbf{T}^{(1)}(\mathbf{q})$ of a single defect [see Eq. (2.51)]; higher-order terms like $\mathbf{T}^{(2)}$ are neglected here. This was calculated by means of the lattice Green's function and a force distribution, which is compatible with the trace of the force dipole tensor.[39,61] Instead of showing $\mathbf{T}^{(1)}(\mathbf{q})$ directly, it is instructive to plot in Fig. 5 the ratio of

$$[|\mathbf{G}_{(330)}\cdot\mathbf{T}^{(1)}_{\text{latt}}(\mathbf{q})|^2+|\mathbf{q}\cdot\mathbf{T}^{(1)}_{\text{latt}}(\mathbf{q})|^2]$$

as calculated properly within the lattice theory, and

$$[|\mathbf{G}_{(330)}\cdot\mathbf{T}^{(1)}_{\text{cont}}(\mathbf{q})|^2+|\mathbf{q}\cdot\mathbf{T}^{(1)}_{\text{cont}}(\mathbf{q})|^2]$$

from the continuum theory [compare Eq. (B1)]. According to Fig. 5 $\mathbf{T}^{(1)}_{\text{cont}}(\mathbf{q})$ remains reliable up to $\frac{1}{5}$ at the maximum wave vector at the zone boundary, which is at $q/G_{110}=0.5$. However, already for q values at half of the Brillouin-zone boundary the continuum theory leads to a serious overestimate of the displacement field.

In niobium the force dipole tensor happens to exhibit cubic symmetry[61] although by symmetry arguments alone the various interstitial sites have only tetragonal symmetry. As a consequence the displacement field happens to be independent from the type α of the interstitial site even for large values of $q=|\mathbf{q}|$:

$$\mathbf{T}^{(1)}_{\alpha}(\mathbf{q})\cong\mathbf{T}^{(1)}(\mathbf{q})\ . \quad (4.2)$$

Thus we obtain

$$\sum_{i,j}(G_iG_j+q_iq_j)C^{(2)}_{ij}(\mathbf{q}) =[|\mathbf{G}\cdot\mathbf{T}^{(1)}(\mathbf{q})|^2+|\mathbf{q}\cdot\mathbf{T}^{(1)}(\mathbf{q})|^2]g(\mathbf{q}) \quad (4.3)$$

with

$$g(\mathbf{q})=\sum_{\alpha,\beta}G^{(2)}_{\alpha-\beta}(\mathbf{q})\ . \quad (4.4)$$

Thus after dividing the experimental data by $[|\mathbf{G}\cdot\mathbf{T}^{(1)}(\mathbf{q})|^2+|\mathbf{q}\cdot\mathbf{T}^{(1)}(\mathbf{q})|^2]$ we finally obtain the Fourier transform of the two-point correlation function averaged over all interstitial sites within a unit cell.

In Fig. 6 $g(\mathbf{q})$ is shown along the $(hh0)$ direction for $Nb_{0.99}Mo_{0.01}D_{0.31}$. One clearly observes the nontrivial correlation effects $g(q)\neq$const. The circles correspond to $T=404$ K, which is still in the one-phase region but only slightly above the coexistence curve (see Fig. 2 and recall the corresponding discussion of the effect of the Mo atoms on the phase diagram). The crosses are the data points for $T=454$ K. This is further away from the coexistence curve and thus the correlation function is reduced. The difference $g(\mathbf{q},T=404\text{ K})-g(\mathbf{q},T=454\text{ K})>0$ is very small at half of the zone boundary but it in-

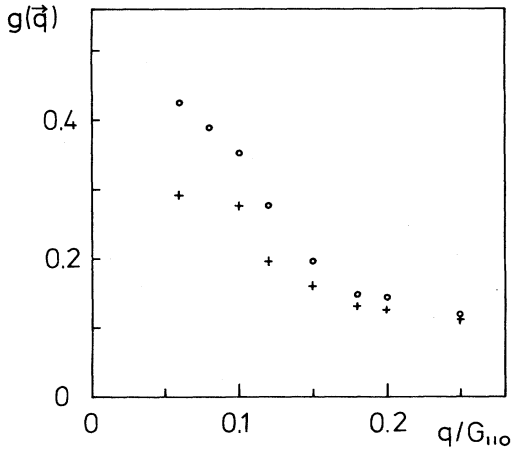

FIG. 6. Fourier transform $g(\mathbf{q})=\sum_{\alpha,\beta}G^{(2)}_{\alpha-\beta}(\mathbf{q})$ of the two-point correlation function, averaged over the interstitial sites α within a unit cell, along the $(hh0)$ direction in reciprocal space for a $Nb_{0.99}Mo_{0.01}D_{0.31}$ alloy. The circles correspond to $T=404$ K, which is slightly above the phase boundary $T_c(x=0.31)$ of this sample. The crosses ($T=454$ K) correspond to a state deeper in the one-phase region.

creases for $q\to 0$. This is in accordance with a system approaching its segregation phase transition. However, in contrast to an ordinary liquid, $g(\mathbf{q}=0)$ does not diverge for $T\to T_c$. As a peculiarity of this lattice gas, $g(\mathbf{q})$ would diverge at the spinodal temperature which is in the two phase region but which is masked by the fact that at T_c the host lattice becomes incoherent.[25]

It is rather instructive to compare the above results with those of $Nb_{0.99}Mo_{0.01}D_{0.06}$ in Fig. 7 along the same direction in reciprocal space. Again the circles ($T=340$ K) correspond to a situation close to the coexistence line,

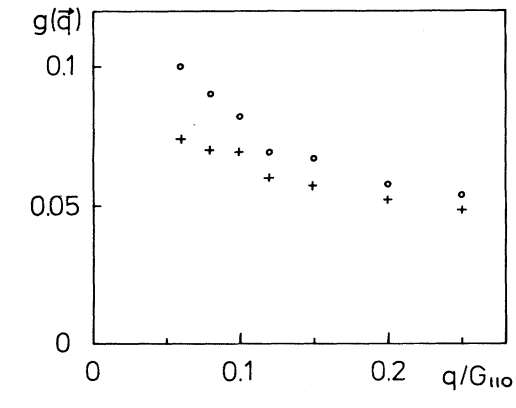

FIG. 7. Fourier transform $g(\mathbf{q})$ of the averaged two-point correlation function along the $(hh0)$ direction in reciprocal space for a $Nb_{0.99}Mo_{0.01}D_{0.06}$ alloy. Again the circles ($T=340$ K) correspond to a state slightly above the phase transition at $T_c(x=0.06)$ and the crosses ($T=470$ K) correspond to a state deeper in the one-phase region. Compared with Fig. 6, here $g(\mathbf{q})$ is smaller and exhibits a weaker q dependence throughout the Brillouin zone.

which for this hydrogen concentration is at lower temperatures (see Fig. 2 and its discussion), and the crosses ($T=470$ K) refer to a state which for $x=0.06$ is well above the solubility limit. Although the general behavior is similar to that in Fig. 6 there are two important differences. First, $g(\mathbf{q})$ in Fig. 7 is much smaller than in Fig. 6. This is mainly due to the reduced hydrogen concentration. According to the crude estimate given in Appendix A one expects that $g(\mathbf{q})\cong x(1-x/x_{\max})$ which is independent both from temperature and $\mathbf{q}$. With $x_{\max}\approx 0.6$ (disregarding the solid phases, see Fig. 2) one would have $g(\mathbf{q},x=0.31)\approx 0.15$ and $g(\mathbf{q},x=0.06)\approx 0.054$. This is rather close to the experimental values of $g(q/G_{110}=0.25)$, which are indeed only weakly temperature dependent. However, due to the cooperative behavior of the interstitials, $g(\mathbf{q})$ exhibits the pronounced temperature dependence for small values of q as discussed above. Second, even for comparable temperatures ($T=454$ K in Fig. 6 and $T=470$ K in Fig. 7) $g(\mathbf{q})$ does not scale simply as $x(1-x/x_{\max})$. For $x=0.06$,

$$\Delta g=\frac{[g(q/G_{110}=0.05)-g(q/G_{110}=0.25)]}{g[q/G_{110}=0.25]}\approx 0.5\ ,$$

whereas for $x=0.31$, $\Delta g\approx 1.5$. Therefore even if one takes the trivial concentration dependence of $g(q)$ into account (on which Δg does no longer depend), for small concentrations $g(\mathbf{q})$ becomes much more plain with respect to its q dependence as compared with higher hydrogen concentrations. The reason for this nontrivial concentration dependence is that the state ($x=0.31$, $T=454$ K) is closer to the phase boundary than the one with ($x=0.06$, $T=470$ K). For very small values of x, $g(\mathbf{q})$ becomes not only very small but also essentially flat, which corresponds to the situation in the fourth group of experiments discussed at the beginning of this section.

This technique can also be exploited in order to follow the influence of the Mo atoms on the two-point correlation function. Figure 8 illustrates this effect for the alloy

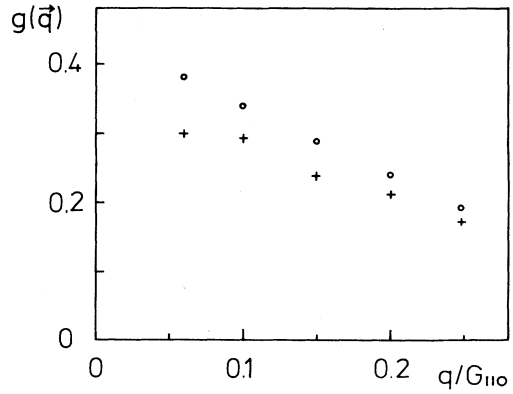

FIG. 8. Fourier transform $g(\mathbf{q})$ of the averaged two-point correlation function along the $(hh0)$ direction in reciprocal space for a $Nb_{0.97}Mo_{0.03}D_{0.30}$ alloy. The circles and crosses correspond to $T=325$ and 452 K, respectively. The increased Mo concentration leads to a different phase separation curve $T_c(x)$ [325 K is again slightly above $T_c(x=0.30)$] and to a different two-point correlation function compared with Figs. 6 and 7.

$Nb_{0.97}Mo_{0.03}D_{0.30}$. By comparing Figs. 6 and 8 one sees that the disorder introduced by the Mo atoms, which are distributed randomly in the Nb matrix, has changed the correlations of the interstitials. The crossover from small- to large-q behavior has become much smoother. A discussion of these effects in terms of a random field can be found in Ref. 64. Here we only want to underscore the possibility of inferring detailed structural information from the distortion-induced diffuse scattering.

In these experiments the antisymmetric part of the Huang diffuse scattering [see Eq. (2.64)] turned out to be an order of magnitude smaller than its corresponding symmetric part. This agrees with our estimates in Appendix B. Therefore the statistical errors of the experimental data presented above did not allow us to extract the three-point correlation function. However, this goal may be within reach in future experiments performed at synchrotron sources.

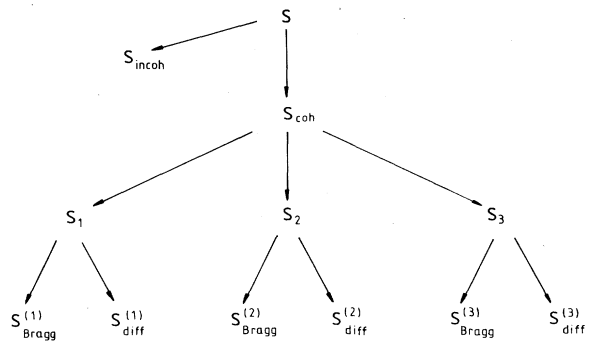

FIG. 9. The total structure factor S splits into the incoherent and coherent part. The latter consists of the scattering at the host lattice (S_1) the Laue contribution (S_2) and the cross term (S_3). All three separate into their diffuse parts and into Bragg peaks, whose intensities are determined by both thermal and static Debye-Waller factors.

V. SUMMARY AND CONCLUSION

In this paper we have analyzed the diffuse scattering of x rays or neutrons at crystals with point defects. We have persued three aims: (i) to express the structure factor systematically in terms of correlation functions of the defect occupation numbers; (ii) to explore the possibility of extracting these correlation functions from scattering data; (iii) to present a successful experimental determination of the two-point correlation function.

The spatial and temporal fluctuations of the defects around their mean concentration lead to local distortions of the host lattice which in turn gives rise to the diffuse scattering of x rays and neutrons. Within the first Born approximation, which is sufficient in the present case, the scattered intensity is proportional to the Fourier transform of the pair correlation in space and time. Thus the position of the displaced scattering centers enter the cross section as arguments of the exponential function. These displacements of the scattering centers depend on the occupation numbers of all interstitial sites, since the displacement field of a defect is long ranged. Therefore the cross section is proportional to the thermal average of a highly nonlinear functional of all interstitial occupation numbers. As a consequence even within the first Born approximation it depends on the *whole hierarchy* of correlation functions (see below).

On the other hand, the cooperative behavior of these interstitial defects may lead to phase transitions, which are of great importance both for practical applications and for basic research. The aforementioned set of correlation functions represents a detailed characterization of these phase transitions. Therefore it is particularly interesting to find a way which allows one to extract at least some of these correlation functions from scattering experiments. In addition they can serve as stringent checks of theoretical predictions for the many-body effects in these systems.

Figure 9 displays the contributions to the dynamic structure factor S. It splits into its coherent part $S_{\rm coh}$ and into its incoherent part $S_{\rm incoh}$. The latter one, which in the case of x-ray scattering contains, e.g., Compton scattering, is not of interest in the present study and will not be discussed in the following. $S_{\rm coh}$ consists of three contributions, S_1, S_2, and S_3. They correspond to the scattering at the host lattice, S_1, and at the interstitials themselves, S_2. S_3 represents the cross term between two scattering amplitudes. S_2 and S_3 are also known as Laue contribution and size-effect term, respectively.

In general all three terms render comparable contributions to the total structure factor S. In such cases it is very difficult to extract precise information about specific correlation functions from the experimental data. Thus x-ray scattering at the important metal-hydrogen systems represents a very favorable situation, because in this case S_2 and S_3 are negligible compared with S_1. On the other hand, neutron scattering at VD_x represents the complementary situation, in which S_1 and S_3 are negligible compared with S_2.

Each of the three terms S_i, $i=1,2,3$, contains both Bragg peaks, $S_{i,\rm Bragg}$, and diffuse scattering contributions $S_{i,\rm diff}$. The strength of the Bragg peaks of the mean-dilated lattice is given *inter alia* by Debye-Waller factors, which are determined by *autocorrelation* functions of the displacement field. Therefore they contain contributions due to both the thermal vibrations and the defect-induced displacements. To lowest order the latter one is given by the integrated two-point correlation function of the occupation numbers of the interstitials weighted by the square of the displacement field of a single defect.

The diffuse scattering intensity yields access to correlations of displacements at *different* sites. There are three reasons why $S_{i,\rm diff}$ depends, even within the first Born approximation, on n-point correlation functions with $n \geq 3$. The first reason is that the probability distribution for the defect-induced displacements is non-Gaussian. Therefore, according to the cumulant expansion, the average over the exponential dependence on the displacement field as described at the beginning of this section leads to the exponential dependence of $S_{i,\rm diff}$ on the sum of n-point

correlation functions whereby all $n \geq 2$ enter. Second, the expansion of this latter exponential in terms of powers of the momentum transfer generates products of higher-order correlation functions of the displacements. As a third reason in general these displacements depend nonlinearly on the occupation numbers.

Figures 10–12 illustrate the dependence of $S_{i,\mathrm{diff}}(\mathbf{q})$ on this hierarchy of correlation functions and thus summarizes our results concerning the first aim (i) (see above). As any arbitrary function, $S_{i,\mathrm{diff}}(\mathbf{q})$ can be separated into a symmetric part $S_{i,\mathrm{sym}}(\mathbf{q})$ and into an antisymmetric part $S_{i,\mathrm{asym}}(\mathbf{q})$. However, the special property of these functions $S_{i,\mathrm{diff}}(\mathbf{q})$ is that, due to the antisymmetry of the displacement field of a single defect, there is a correspondence between the order of the correlation functions entering these expressions and their symmetry: $S_{1,\mathrm{sym}}$ and $S_{2,\mathrm{sym}}$ are given by correlation functions of even order, whereas $S_{1,\mathrm{asym}}$ and $S_{2,\mathrm{asym}}$ are determined by odd correlation functions. In the cross term the situation is reversed: The symmetric part $S_{3,\mathrm{sym}}$ is given by odd correlation functions and the antisymmetric part follows from even correlation functions.

In Figs. 10–12 the third level from above ($S_{i,\mathrm{diff}}$ represents the top level) indicates those displacement correlation functions on which $S_{i,\mathrm{sym}}$ and $S_{i,\mathrm{asym}}$, respectively, depend. In the level below one sees how these correlation functions are composed of those corresponding to thermal vibrations and defect-induced displacements, respectively. *Inter alia*, the former ones make up the thermal diffuse scattering as present in the perfect lattice. [Here the thermal vibrations are taken to be statistically independent from the defect-induced displacements. Experimental data support this approximation (see Fig. 1).] In the next level below we have placed all those correlation functions of the occupation numbers, which follow from the aforementioned correlation functions due to linear terms in the dependence of the displacements on the occupation numbers. In the next level and in those indicated by dots we placed all those correlation functions which are generated additionally by the bilinear and higher-order terms, respectively, in this dependence.

In view of this classification scheme we are now in the position to persue our second aim (ii) (see above), i.e., to analyze the possibility of extracting various correlation functions from the experimental data. Here we focus on the aforementioned cases in which the total structure factor is dominated either by S_1 or by S_2. (The more general case, as it occurs in binary alloys, will be discussed later.)

First consider the directly accessible Bragg peak intensity. By taking the ratio between the scattering intensities stemming from the crystal with and without defects, respectively, one gets rid of the thermal Debye-Waller factor and obtains the defect-induced static Debye-Waller factor. As described above, this measures the integrated and weighted two-point correlation function $\langle \tau^2 \rangle$ of the defects as long as higher terms remain negligible. (Here and in the following $\langle X^m \rangle$ is the short notation for an

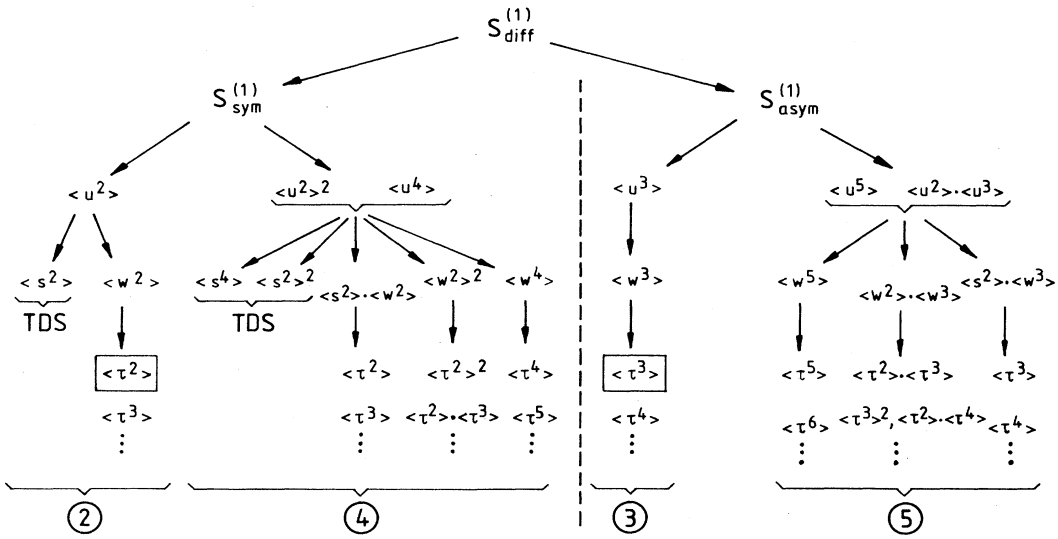

FIG. 10. Hierarchy of correlation functions determining the diffuse scattering at the host lattice. The even (2,4,...) correlation functions are symmetric, whereas the odd ones (3,5,...) are antisymmetric around the Bragg peak. $u = w + s$ denotes the total displacement field composed of thermal vibrations s and defect-induced distortions w. Here, w and s are assumed to be statistical independent. $\langle X^m \rangle^n$ denotes the product of n m-point correlation functions of the variable X. Correlation functions involving only $X = s$ represent the so-called thermal diffuse scattering TDS. Products of correlation functions of s with those of w might also be attributed to TDS. Those terms of w, which are linear in the occupation numbers τ, give rise to the first line of correlation functions of τ, whereas those in the second line are due to the second-order terms of $w\{\tau\}$; the dots indicate even higher-order terms [see Eq. (2.51)]. As discussed in Secs. II and V those correlation functions in the box are experimentally accessible; the other ones are subdominant (see Appendix B). A product of k factors τ, l factors w, and m factors s is regarded as a $(k+l+m)$-point correlation function.

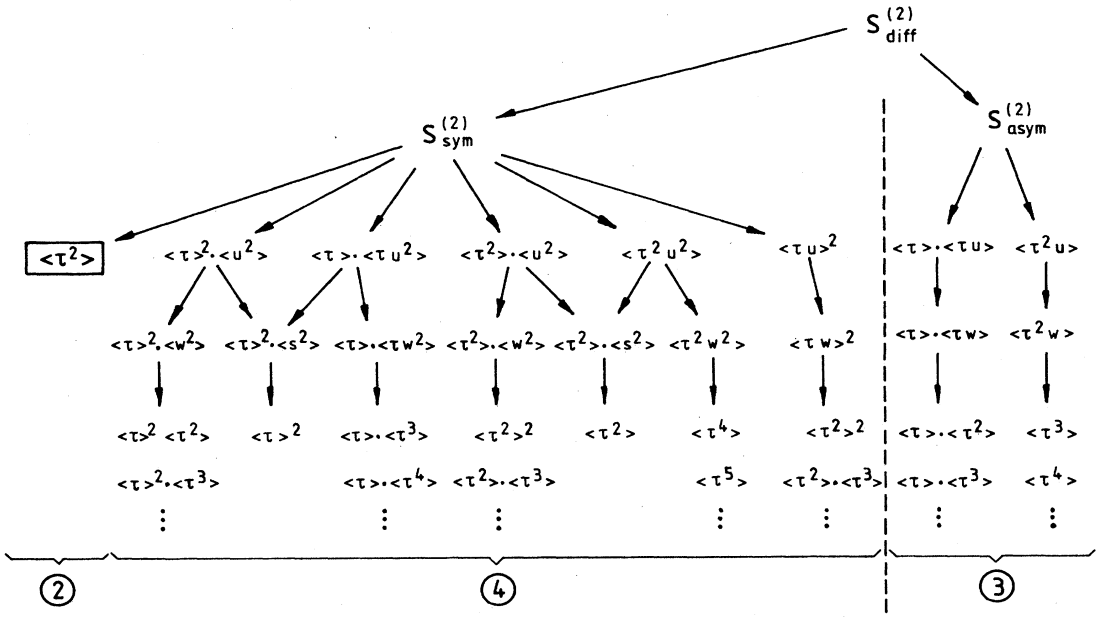

FIG. 11. Hierarchy of correlation functions entering the Laue contribution. We use the same notation as in Fig. 10. Note that here as in Fig. 10 the symmetric part is determined by even (2,4,. . .) correlation functions and the antisymmetric part by odd ones (3,. . .). For reasons of tranparency we omitted 5. In $2\langle\tau^2\rangle$ enters without displacement fields. But only in small angle scattering does it represent the leading contribution. Otherwise it is dominated by $\langle\tau^2\rangle\langle w^2\rangle$ and $\langle\tau^2\rangle\langle s^2\rangle$ (see Sec. III) appearing in 4.

m-point correlation function of the variable X.)

In the next step let us consider $S_{1,\mathrm{sym}}$, which can be constructed directly from the experimental data by taking $[S(\mathbf{q})+S(-\mathbf{q})]/2$. According to Fig. 10 this eliminates all odd correlation functions. In order to obtain the momentum dependence of the two-point correlation function, i.e., $\langle\tau^2\rangle$, two steps are required. First, by taking carefully the difference between the scattering intensities of the crystal with and without defects one obtains the Fourier transform of the sum of all those even correlation functions, which are *not* due to the thermal diffuse scattering (TDS) (compare the fourth level in Fig. 10). Second, by calculating approximately the various four-point correlation functions of the displacements one finds that ordinarily their contribution is small compared with that of the two-point correlation function $\langle w^2\rangle$. Conse-

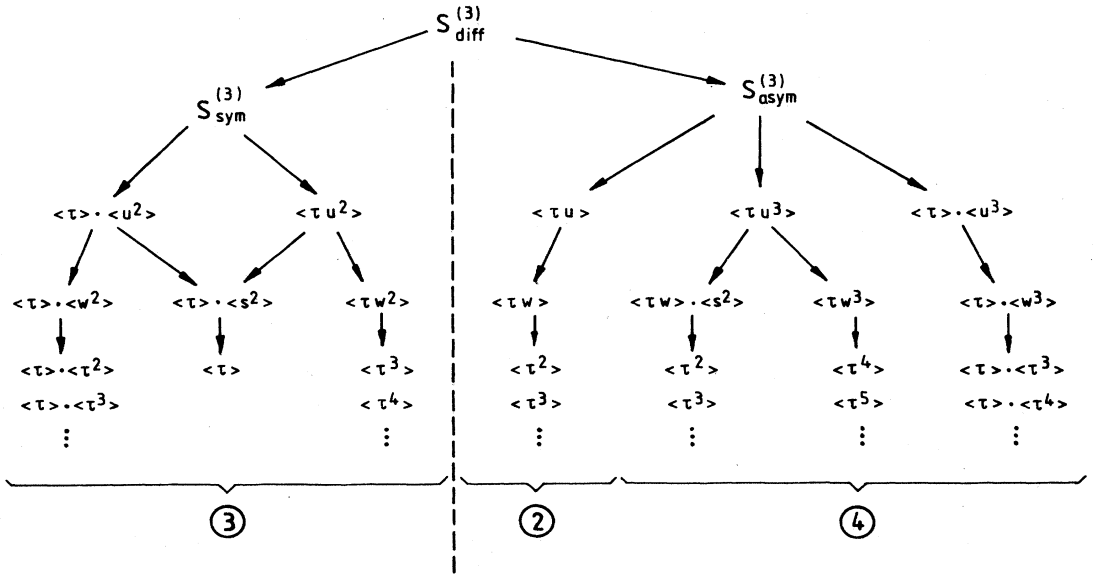

FIG. 12. Hierarchy of correlation functions determining the cross term S_3. We use the same notation as in Figs. 10 and 11. Note, however, that in contrast to $S_{1,\mathrm{diff}}$ and $S_{2,\mathrm{diff}}$, here the symmetric part is determined by odd correlation functions (3,. . .) and the antisymmetric part by even ones (2,4,. . .). Again we omit 5.

quently the procedure described above yields the two-point correlation function of the occupation numbers, i.e., $\langle \tau^2 \rangle$, after applying theoretical results for the displacement field of a single defect. As an alternative one can determine this displacement field experimentally by using scattering data from a sample with a very low hydrogen concentration. In this case $\langle \tau_a \tau_b \rangle_c = c$ with high accuracy which in turn allows one to determine the displacement field of a single defect. This result can be applied for higher values of c, for which $\langle \tau_a \tau_b \rangle_c$ is not known.

The fact that $\langle w^2 \rangle$ yields directly $\langle \tau^2 \rangle$ is only correct as long as the nonlinear terms in the relationship between the displacements and the occupation numbers are negligible, which should be fulfilled for not too high defect concentrations. This seems to be supported by the experimental observation that the lattice constant of the host lattice varies linearly with the defect concentration.

According to Fig. 10 the antisymmetric part $S_{1,\mathrm{asym}} = [S_1(\mathbf{q}) - S_1(-\mathbf{q})]/2$ does not contain any thermal diffuse scattering. This reflects the symmetric probability distribution of the thermal vibrations due to their statistical independence from the defect-induced displacements. In analogy to the structure of $S_{1,\mathrm{sym}}$, here the smallness of the five-point correlation functions leads us to the conclusion that $S_{1,\mathrm{asym}}$ is determined by the three-point correlation function $\langle \tau^3 \rangle$ and the displacement field of a single defect, whereby the latter one may be taken from theoretical calculations. Since there is only a single scattering momentum $\mathbf{q}$ and because the Fourier transform $\langle \tau^3 \rangle$ depends on two momenta, the experimental data can uniquely determine only a partial trace of $\langle \tau^3 \rangle$. But this still represents a very detailed information going beyond that one of $\langle \tau^3 \rangle$, which would follow from studying the pressure dependence of $\langle \tau^2 \rangle$. There are two possibilities how this information can be exploited. In the first one these experimental data can be checked against theoretical predictions for the three-point correlation functions as obtained, e.g., from Monte-Carlo calculations. This is a rather sensitive test, because one is still left with one full $\mathbf{q}$ dependence. The second possibility resorts to experimental data alone. By taking the results for $\langle \tau^2 \rangle$ as obtained from $S_{1,\mathrm{sym}}$ one can check how good $\langle \tau^3 \rangle$ is approximated by the Kirkwood approximation, which expresses $\langle \tau^3 \rangle$ in terms of $\langle \tau^2 \rangle$. The original Kirkwood approximation, which plays an important role in the theory of dense liquids and for the solid-liquid phase transition of ordinary liquids, is supposed to be reliable for large distances between all correlated sites but it breaks down at small distances. Since the interstitials represent a *lattice gas* without double occupancy (i.e., $\tau_a^2 = \tau_a$), its three-point correlation function exactly reduces to a two-point correlation function as soon as any two of its three sites coincide. Thus in the present case one can apply a *modified Kirkwood approximation,* which retains the merits of the original one but which in addition becomes an exact relation at short distances. This kind of analysis is in contrast to the scattering at ordinary liquids, which is isotropic and which therefore does not allow one to separate even from odd correlation functions on the basis of symmetry arguments as we can do here. Thus for those systems the Kirkwood approximation can be tested only by using numerical calculations. Here, however, one can test it on the basis of one and the same scattering data. Therefore the antisymmetric part of x-ray scattering intensities at metal-hydrogen systems offers a unique experimental test of approximation schemes in statistical mechanics.

The experimental data presented in Sec. IV realize the first part of this envisaged analysis. Following the above procedure the x-ray scattering data from $\mathrm{Nb}_{1-y}\mathrm{Mo}_y\mathrm{D}_x$ systems yield the Fourier transform of the two-point correlation function for various values of $y \ll 1$, x, and temperature along a certain direction in the Brillouin zone. As discussed in Sec. IV these results for $\langle \tau^2 \rangle$ reflect nicely the gas-liquidlike phase transition of the dissolved interstitials and opens the door for quantitative tests of model calculations. In accordance with our estimates the antisymmetric part of the diffuse scattering intensity is about an order of magnitude smaller than the symmetric part. Unfortunately, with respect to this antisymmetric part, the resulting statistical errors of the presently available experimental data are rather large and therefore do not allow us to present a sound analysis of the three-point correlation function $\langle \tau^3 \rangle$ as outlined above. This is left to future possible experiments at synchrotron sources.

Let us now turn to those systems and scattering processes, which yield S_2 instead of S_1. The notable difference is that $\langle \tau^2 \rangle$ enters into S_2 both directly and indirectly via the displacement correlations (see Fig. 11). However, with exception of the forward direction, the latter contribution dominates due to its q^{-2} divergence, whereas $\langle \tau^2 \rangle$ remains finite for $q \to 0$. Even in the forward direction, where the contributions from the displacements do not diverge for $q \to 0$, it is difficult to determine $\langle \tau^2 \rangle$, because the thermal diffuse scattering can no longer be separated by comparing the crystal with and without defects: S_2 vanishes $\propto \langle \tau \rangle^2$ for $\langle \tau \rangle \to 0$. Thus one must resort to inelastic measurements in order to isolate the thermal diffuse contribution on the basis of its characteristic frequency and momentum dependence. This represents a rather subtle problem, whose solution seems to be more complicated than the analysis of those systems with scattering intensities determined by S_1.

Naturally the cross term S_3 (see Fig. 12) cannot be determined separately. If S_2 is negligible compared with S_1, S_3 represents the first correction term for S_1 but it remains subdominant. The same is true if S_1 is small compared with S_2. However, with exception of these special cases, S_3 is in general of the same importance as S_1 and S_2.

ACKNOWLEDGMENTS

It is a pleasure for us to acknowledge numerous fruitful discussions with Professor S. C. Moss, Professor J. Peisl, and Professor H. Wagner as well as their continuing support and encouragement. This work has been supported by the Bundesministerium für Forschung und Technologie under Grant No. 03WA1LMU/5.

APPENDIX A

At high temperatures the interstitials are only weakly correlated, i.e., approximately $\{\tau_a\}$ forms a set of statistically independent variables. Consequently, the correlation functions factorize in this limit. However, even at relatively high temperatures this is not completely true, since up to the melting point of the host lattice the interstitial sites can be occupied only by a single particle. Thus, in the simplest nontrivial approximation, one treats $\{\tau_a\}$ as independent variables but keeps the condition $\tau_a^n=\tau_a$ for $n=1,2,\ldots$. With some combinatorics one finds for the first four correlation functions

$$\langle\tau_a\rangle=c_\alpha,\quad \langle\tau_b=\rangle=c_\beta,\quad \langle\tau_c\rangle=c_\gamma\ , \tag{A1}$$

$$\langle\tau_a\tau_b\rangle=c_\alpha c_\beta+c_\alpha(1-c_\alpha)\delta_{a,b}\ , \tag{A2}$$

$$\begin{aligned}\langle\tau_a\tau_b\tau_c\rangle=&c_\alpha c_\beta c_\gamma+c_\alpha(1-c_\alpha)c_\gamma\delta_{a,b}\\&+c_\beta(1-c_\beta)c_\alpha\delta_{b,c}+c_\alpha(1-c_\alpha)c_\beta\delta_{a,c}\\&+c_\alpha(1-c_\alpha)(1-2c_\alpha)\delta_{a,b}\delta_{b,c}\ ,\end{aligned} \tag{A3}$$

and

$$\begin{aligned}\langle\tau_a\tau_b\tau_c\tau_d\rangle=&c^4+c^3(1-c)(\delta_{a,b}+\delta_{a,c}+\delta_{a,d}+\delta_{b,c}+\delta_{b,d}+\delta_{c,d})\\&+c^2(1-c)(1-2c)(\delta_{a,b}\delta_{b,c}+\delta_{a,b}\delta_{b,d}+\delta_{b,c}\delta_{c,d}+\delta_{c,d}\delta_{a,c})\\&+c^2(1-c)^2(\delta_{a,b}\delta_{c,d}+\delta_{a,d}\delta_{b,c}+\delta_{a,c}\delta_{b,d})+c(1-c)(1-6c+6c^2)\delta_{a,b}\delta_{b,c}\delta_{c,d}\ .\end{aligned} \tag{A4}$$

In Eq. (A4) we have assumed for reasons of simplicity that $\langle\tau\rangle=c$ for all types of interstitial sites. Equations (A1)–(A4) represent grand canonical correlation functions. It will turn out (see Appendix B) that within this approximation only the last terms of Eq. (A2) and (A3) and the last two terms of Eq. (A4) lead to nonvanishing contributions to the displacement correlation functions entering the cross section. Note that these contributions are symmetric functions of c around $c=\frac{1}{2}$ displaying the particle-hole symmetry $\tau_a\leftrightarrow 1-\tau_a$ of the underlying microscopic Hamiltonian of the interstitial defects. In reality the repulsive part of the interaction energy between two interstitial defects is not restricted to a single site so that the maximum concentration $c_{\max}$ is less than 1. Approximately this effect could be incorporated into Eqs. (A1)–(A4) in replacing $1-c$ by $1-(c/c_{\max})$. Within this approximation the cumulants are

$$\langle\tau_a\rangle_c=c_\alpha\ , \tag{A5}$$

$$\langle\tau_a\tau_b\rangle_c=c_\alpha(1-c_\alpha)\delta_{a,b}\ , \tag{A6}$$

$$\langle\tau_a\tau_b\tau_c\rangle_c=c_\alpha(1-c_\alpha)(1-2c_\alpha)\delta_{a,b}\delta_{b,c}\ , \tag{A7}$$

and

$$\langle\tau_a\tau_b\tau_c\tau_d\rangle_c=c_\alpha(1-c_\alpha)(1-6c_\alpha+6c_\alpha^2)\delta_{a,b}\delta_{b,c}\delta_{c,d}\ . \tag{A8}$$

APPENDIX B

In this appendix we present approximate expressions for the static displacement correlation functions $C^{(n)}$. They exhibit the general structure of the various terms entering the cross section in Eq. (2.41) and they allow one to estimate their relative importance quantitatively. We make the following approximations.

(i) The correlation functions $G^{(n)}$ of the occupation numbers are taken as in Eqs. (A1)–(A4) disregarding the difference between the $n_{\rm H}$ different interstitial sites within a unit cell.

(ii) The asymptotic form of the displacement field $\mathbf{T}^{(1)}$ [Eq. (2.61)] is used throughout the Brillouin zone, which is taken to be a sphere of radius

$$q_{\max}=(6\pi^2)^{1/3}V_{\rm cell}^{-1/3}\ .$$

In real space

$$\mathbf{T}^{(1)}(\mathbf{r})=P[4\pi(c_{12}+2c_{44})]^{-1}\mathbf{r}/r^3\ . \tag{B1}$$

(iii) We replace lattice sums by integrals. In some cases this leads to artificial divergencies due to the extrapolation of the asymptotic behavior of $\mathbf{T}^{(1)}$ at large distances down to small values of r, where $\mathbf{T}^{(1)}$ should be substituted by its proper lattice form. We avoid these divergences by using the lattice constant as a lower cutoff such that $\mathbf{T}^{(1)}(r)=\mathbf{0}$ for $r<a$.

Approximations (ii) and (iii) can be dropped by using the lattice version of $\mathbf{T}^{(1)}$. We avoid the corresponding numerical calculation, which can be performed for specific host lattices (see Sec. IV and Fig. 5), because we are interested in estimates for the *relative* strengths of various terms and because we want to adhere to rather general expressions.

Thus with Eqs. (2.44)–(2.48), (2.51), and (B1) and with the dimensionless abbreviation

$$A=P[4\pi V_{\rm cell}(c_{12}+2c_{44})]^{-1} \tag{B2}$$

we obtain the following expressions:

$$\begin{aligned}C_{ij}^{(2)}(\mathbf{R})=&c(1-c)n_{\rm H}V_{\rm cell}A^2(\partial/\partial R_i)\\&\times\int d^3r(r_j/r^3)|\mathbf{r}-\mathbf{R}|^{-1}\\=&2\pi c(1-c)n_{\rm H}V_{\rm cell}A^2(\delta_{ij}-E_iE_j)/R\end{aligned} \tag{B3}$$

and

$$C_{ij}^{(2)}(\mathbf{q})=(4\pi)^2c(1-c)n_{\rm H}A^2(e_ie_j)/q^2\ . \tag{B4}$$

$\mathbf{E}=\mathbf{R}/R$ and $\mathbf{e}=\mathbf{q}/q$ denote unit vectors. The integral in Eq. (B3) can be evaluated straightforwardly by expanding $|\mathbf{r}-\mathbf{R}|^{-1}$ into spherical harmonics.

For the higher-order correlation functions we focus on the behavior of large R and small q, respectively, where Eqs. (2.61) and (B1) hold. Thus we obtain [see Eq. (2.62)]

$$C_{ijk}^{(3)}(\mathbf{q})=n_{\mathrm{H}}c(1-c)(1-2c)T_k^{(1)}(-\mathbf{q})\int d^3q'\,T_i^{(1)}(\mathbf{q}')T_j^{(1)}(\mathbf{q}-\mathbf{q}')$$
$$\rightarrow -i(32\pi/3)(6\pi^2)^{1/3}c(1-c)(1-2c)n_{\mathrm{H}}A^3V_{\mathrm{cell}}^{2/3}\delta_{ij}e_k/q\ , \tag{B5}$$

and by Fourier transformation

$$C_{ijk}^{(3)}(\mathbf{R})\cong -\tfrac{8}{3}(6\pi^2)^{1/3}c(1-c)(1-2c)n_{\mathrm{H}}A^3V_{\mathrm{cell}}^{5/3}\delta_{ij}E_k/R^2\ . \tag{B6}$$

The next term in Eq. (2.41) is basically the Fourier transform of the square of the two-point correlation function,

$$C_{ijkl}^{(4,0)}(\mathbf{R})=C_{ij}^{(2)}(\mathbf{R})C_{kl}^{(2)}(\mathbf{R})$$
$$\cong 4\pi^2c^2(1-c)^2n_{\mathrm{H}}^2V_{\mathrm{cell}}^2A^4(\delta_{ij}\delta_{kl}-\delta_{ij}E_kE_l-\delta_{kl}E_iE_j+E_iE_jE_kE_l)(1/R^2)\ , \tag{B7}$$

and thus a tedious calculation gives

$$C_{ijkl}^{(4,0)}(\mathbf{q})=\int d^3q'\,C_{ij}^{(2)}(\mathbf{q}')C_{kl}^{(2)}(\mathbf{q}-\mathbf{q}')$$
$$\cong \pi^4c^2(1-c)^2n_{\mathrm{H}}^2V_{\mathrm{cell}}A^4[(\delta_{ij}\delta_{kl}+\delta_{ik}\delta_{jl}+\delta_{il}\delta_{jk})$$
$$-(\delta_{ik}e_je_l+\delta_{il}e_je_k+\delta_{jk}e_ie_l+\delta_{jl}e_ie_k)+3(\delta_{ij}e_ke_l+\delta_{kl}e_ie_j+e_ie_je_ke_l)](1/q)\ . \tag{B8}$$

The expression for the first true four-point correlation function reads

$$C_{ijkl}^{(4,1)}(\mathbf{R})=c(1-c)(6c^2-6c+1)n_{\mathrm{H}}V_{\mathrm{cell}}^3A^4I_{ijkl}^{(1)}(\mathbf{R}) \tag{B9}$$

with

$$I_{ijkl}^{(1)}(\mathbf{R})=\int d^3r[(\mathbf{r}+\mathbf{R})_i(\mathbf{r}+\mathbf{R})_jr_kr_l]/(|\mathbf{r}+\mathbf{R}|^6r^6)\ . \tag{B10}$$

The integrand in Eq. (B10) is peaked at $\mathbf{r}=\mathbf{0}$ and $\mathbf{r}=-\mathbf{R}$ so that

$$I_{ijkl}^{(1)}(\mathbf{R})\cong \int d^3r(R_iR_jr_kr_e)/(R^6r^6)+\int d^3r[(\mathbf{r}+\mathbf{R})_i(\mathbf{r}+\mathbf{R})_j(-\mathbf{R})_k(-\mathbf{R})_l]/(|\mathbf{r}+\mathbf{R}|^6R^6)\ . \tag{B11}$$

The integrals in Eq. (B11) are regularized at $\mathbf{r}=\mathbf{0}$ and $\mathbf{r}=-\mathbf{R}$ as described above [see (iii)]. $I^{(1)}(\mathbf{R})$ can also be expressed in terms of partial derivatives with respect to R_i and R_j of integrals involving $|\mathbf{r}-\mathbf{R}|^{-2}$ and $|\mathbf{r}-\mathbf{R}|^{-4}$, respectively. These functions can be completely factorized by an expansion in terms of Gegenbauer polynomia, which can then be integrated term by term. This approach shows that Eq. (B11) captures the correct behavior of $I^{(1)}(\mathbf{R})$ for large R. Therefore we end up with

$$C_{ijkl}^{(4,1)}(\mathbf{R})\cong(4\pi/3)c(1-c)(6c^2-6c+1)n_{\mathrm{H}}V_{\mathrm{cell}}^3a^{-1}A^4(\delta_{ij}E_kE_l+\delta_{kl}E_iE_j)(1/R^4) \tag{B12}$$

and correspondingly in Fourier space

$$C_{ijkl}^{(4,1)}(\mathbf{q})\cong(\pi^2/12)c(1-c)(6c^2-6c+1)n_{\mathrm{H}}(V_{\mathrm{cell}}/a)^2A^4\{(32/3\pi)\delta_{ij}\delta_{kl}-[2\delta_{ij}\delta_{kl}+\delta_{ij}e_ke_l+\delta_{kl}e_ie_j](qa)\}\ . \tag{B13}$$

Whereas the contribution $\sim q$ reflects correctly the asymptotic behavior of $C^{(4,1)}(R)$ for large R, $C^{(4,1)}(\mathbf{q}=\mathbf{0})$ will be modified by the higher-order terms which have been neglected in Eq. (B12).

Finally the last contribution due to four-point correlation functions is

$$C_{ijkl}^{(4,2)}(\mathbf{R})=c(1-c)(6c^2-6c+1)n_{\mathrm{H}}V_{\mathrm{cell}}^3A^4(\partial/\partial R_l)I_{ijk}^{(2)}(\mathbf{R}) \tag{B14}$$

with

$$I_{ijk}^{(2)}(\mathbf{R})=\int d^3r(r_ir_jr_k)/(r^9|\mathbf{r}-\mathbf{R}|)\ . \tag{B15}$$

Again by factorizing $|\mathbf{r}-\mathbf{R}|^{-1}$ in terms of spherical harmonics $I^{(2)}$ can be calculated exactly. After a lengthy calculation one obtains

$$I_{ijk}^{(2)}(\mathbf{R})=[2\pi/(15a^2)](\delta_{ij}E_k+\delta_{ik}E_j+\delta_{jk}E_i)\cdot(1/R^2)+(4\pi/7)[E_iE_jE_k-\tfrac{1}{5}(\delta_{ij}E_k+\delta_{ik}E_j+\delta_{jk}E_i)][\ln(R/a)]/R^4$$
$$+(4\pi/7)[\tfrac{1}{7}E_iE_jE_k-\tfrac{17}{50}(\delta_{ij}E_k+\delta_{ik}E_j+\delta_{jk}E_i)](1/R^4)\ . \tag{B16}$$

To leading order one finds, therefore,

$$C_{ijkl}^{(4,2)}(\mathbf{R})\cong(2\pi/15)c(1-c)(6c^2-6c+1)n_{\mathrm{H}}V_{\mathrm{cell}}^3a^{-2}A^4[\delta_{ij}(\delta_{kl}-3E_kE_l)+\delta_{ik}(\delta_{jl}-3E_jE_l)+\delta_{jk}(\delta_{il}-3E_iE_l)]1/R^3 \tag{B17}$$

and in Fourier space

$$C_{ijkl}^{(4,2)}(\mathbf{q})\cong(8\pi^2/15)c(1-c)(6c^2-6c+1)n_{\mathrm{H}}(V_{\mathrm{cell}}/a)^2A^4[\delta_{ij}e_le_k+\delta_{ik}e_je_l+\delta_{jk}e_ie_l-\tfrac{1}{3}(\delta_{ij}\delta_{lk}+\delta_{ik}\delta_{jl}+\delta_{jk}\delta_{il})]\ . \tag{B18}$$

As before, the nonanalytic contributions in Eq. (B18), i.e., $\sim e_l e_k$, etc., reflect correctly the asymptotic behavior of $C^{(4,2)}(\mathbf{R})$ for large R, whereas the contribution in the square brackets will be modified by higher-order terms omitted in Eq. (B17). Note that $C^{(4,1)}(\mathbf{R})$ decays more rapidly ($\sim R^{-4}$) than $C^{(4,2)}(\mathbf{R}) \sim R^{-3}$, so that one could expect a logarithmic divergence of $C^{(4,2)}(\mathbf{q}\to\mathbf{0})$. However, the angular dependence of $C^{(4,2)}(\mathbf{R})$ is such, that $C^{(4,2)}(\mathbf{q})$ remains finite for $\mathbf{q}\to\mathbf{0}$. Both $C^{(4,1)}(\mathbf{q})$ and $C^{(4,2)}(\mathbf{q})$ are nonanalytic at $\mathbf{q}=\mathbf{0}$. Their slope and their value at $\mathbf{q}=\mathbf{0}$, respectively, depend on the choice of the path approaching the center of the Brillouin zone.

Since the true four-point correlation functions $C^{(4,1)}$ and $C^{(4,2)}$ remain finite at $\mathbf{q}=\mathbf{0}$, one finds that for small q the contribution $\propto K^4$ in the cross section [Eq. (2.41)] is dominated by the square of the two-point correlation function $C^{(4,0)}(\mathbf{q}) \sim q^{-1}$. Although its angular dependence is rather different $C^{(3)}(\mathbf{q})$ shows the same type of divergence $\sim q^{-1}$.

Collecting the various terms the diffuse part of the cross section within our approximation and close to the Bragg peak now reads [the terms correspond to their counterparts in Eq. (2.41)]

$$S_{1,\mathrm{diff}}(\mathbf{K}) = N_L |f_{\mathrm{at}}(\mathbf{G})|^2 e^{-2W(\mathbf{G})} \times \{H_2 + H_3 + H_{4,0} + H_{4,1} + H_{4,2} + \cdots\} \tag{B19}$$

with

$$H_2(\mathbf{G},\mathbf{q}) = 16\pi^2 c(1-c) n_{\mathrm{H}} (A\bar{G})^2 (\cos^2\alpha) \bar{q}^{-2} , \tag{B20}$$

$$H_3(\mathbf{G},\mathbf{q}) = \tfrac{32}{3}(6\pi^5)^{1/3} c(1-c)(1-2c) \times n_{\mathrm{H}} \bar{V}_{\mathrm{cell}}^{2/3} (A\bar{G})^3 (\cos\alpha) \bar{q}^{-1} , \tag{B21}$$

$$H_{4,0}(\mathbf{G},\mathbf{q}) = \tfrac{3}{2}\pi^4 c^2 (1-c)^2 n_{\mathrm{H}}^2 \bar{V}_{\mathrm{cell}} (A\bar{G})^4 \times (1+\cos^2\alpha+\cos^4\alpha) \bar{q}^{-1} , \tag{B22}$$

$$H_{4,1}(\mathbf{G},\mathbf{q}) = (\pi^2/24) c(1-c)(6c^2-6c+1) n_{\mathrm{H}} \bar{V}_{\mathrm{cell}}^2 \times (A\bar{G})^4 [(16/3\pi) - (1+\cos^4\alpha)\bar{q}] , \tag{B23}$$

and

$$H_{4,2}(\mathbf{G},\mathbf{q}) = (8\pi^2/15) c(1-c)(6c^2-6c+1) n_{\mathrm{H}} \times \bar{V}_{\mathrm{cell}}^2 (A\bar{G})^4 (\tfrac{1}{3} - \cos^4\alpha) . \tag{B24}$$

Here we have introduced reduced units $\bar{V}_{\mathrm{cell}} = V_{\mathrm{cell}}/a^3$, $\bar{G} = Ga$, and $\bar{q} = qa$; α denotes the angle between $\mathbf{G}$ and $\mathbf{q}$, $\cos\alpha = \mathbf{G}\cdot\mathbf{q}/(Gq)$.

Due to the dipolar character of the displacement field H_2 and H_3 vanish in leading order if $\mathbf{G}$ and $\mathbf{q}$ are orthogonal, but $H_{4,i}$ do not vanish. In particular one is left in this case with a $\bar{q}^{-1}$ divergence stemming from the square of the two-point correlation function [see Eq. (B22)].

The relative strength of the terms in Eqs. (B20)–(B24) depends mainly on the dimensionless parameter $A\bar{G}$ and the $\bar{q}$ dependence. In order to get a quantitative estimate let us consider the particular system NbH_x. Thus we have $\bar{V}_{\mathrm{cell}} = 1/2$, $n_{\mathrm{H}} = 6$, and $a = 3.3$ Å. With $P = \frac{10}{3}$ eV, $c_{12} = 1.35\times10^{12}$ dyn/cm^2, and $c_{44} = 0.29\times10^{12}$ dyn/cm^2, we have $A = 1.22\times10^{-2}$. For the (110) reflex $\bar{G} = 8.89$ whereas $\bar{G} = 26.66$ for the (330) reflex. Thus $A\bar{G}_{(110)} = 0.108$ and $A\bar{G}_{(330)} = 0.325$, respectively. Therefore we obtain for the (110) Bragg reflex ($\mathbf{q}\to-\mathbf{q}$ implies $\cos\alpha\to-\cos\alpha$)

$$H_2 = 11\{100\} c(1-c)(\cos^2\alpha)\bar{q}^{-2} , \tag{B25}$$

$$H_3 = 0.62\{17\} c(1-c)(1-2c)(\cos\alpha)\bar{q}^{-1} , \tag{B26}$$

$$H_{4,0} = 0.36\{29\} c^2(1-c)^2(1+\cos^2\alpha+\cos^4\alpha)\bar{q}^{-1} , \tag{B27}$$

$$H_{4,1} = 1.4\times10^{-4}\{1.2\times10^{-2}\} \times c(1-c)(6c^2-6c+1) , \tag{B28}$$

$$H_{4,2} = 3.6\times10^{-4}\{2.9\times10^{-2}\} \times c(1-c)(6c^2-6c+1)(1-3\cos^4\alpha) . \tag{B29}$$

The prefactors in curly brackets correspond to the (330) reflex. The estimates in Eqs. (B25)–(B29) confirm our statement in the main text that the symmetric part of the diffuse scattering intensity, i.e., $H_2 + \sum_i H_{4,i} + \ldots$, is dominated by the contribution from the two-point correlation function, i.e., by H_2. At least for small values of $\bar{q}$ and $\alpha \neq 90°$ this is always true because H_2 exhibits the strongest divergence. Moreover, if $A\bar{G} < 1$ as in the above examples, even the prefactors favor H_2. However, this is no longer true for reflexes of very high order for which $A\bar{G}$ may become larger than 1. In these cases and for larger values of $\bar{q}$ the contributions of the higher-order correlation functions can no longer be neglected.

Although we did not calculate explicitly the various five-point correlation functions, which represent the first correction terms to H_3 in the antisymmetric part of the section, we expect them to remain finite at $\mathbf{q}=\mathbf{0}$. Since H_3 and H_5 differ by a factor $(A\bar{G})^2$, basically the same arguments as above for H_2 and H_4 apply here, too.

Near $\alpha = 90°$ (and 270°) these remarks are no longer valid, since there H_2 and H_3 vanish to leading order and $H_{4,0}$ starts to play an important role. Since for $\alpha\to90°$ H_2 vanishes more rapidly than H_3 the asymmetry of the cross section is relatively enhanced in these orthogonal directions.

The concentration dependence of the H_n deserves a few remarks. Within our crude approximation the H_n vanish for $c=0$ and $c=1$ and they are symmetric around $c=\frac{1}{2}$. With the exception of $H_{4,0}$ all contributions are $\sim c$ for $c\to0$. Since $H_{4,0}$ stems from the square of the two-point correlation function one has $H_{4,0}\sim c^2$ for $c\to0$. Thus for a small hydrogen concentration $H_{4,0}$ is substantially decreased with respect to the other contributions. This further justifies the statement that the symmetric part of the cross section is dominated by H_2. Finally note that the contributions of the higher-order correlation functions may vanish at certain hydrogen concentrations: Within our approximation $H_3 = 0$ for $c=\frac{1}{2}$ and $H_{4,1} = H_{4,2} = 0$ for $c = (1/2) - 1/\sqrt{12}$ and $c = (1/2) + 1/\sqrt{12} = 0.79$, respectively.

Thus putting aside special situations we can conclude that for Bragg peaks of low order the symmetric part of

the diffuse scattering is dominated by the two-point correlation function and the antisymmetric part by the three-point correlation function.

APPENDIX C

In this appendix we discuss a thermodynamic relationship between the three-point and the two-point correlation functions.

The host lattice provides an effective Hamiltonian $H\{\tau\}$ for the interstitial atoms. Their thermodynamic behavior follows from the grand canonical partition function [$\beta=(k_BT)^{-1}$]

$$Z(T,V,\mu)=\sum_{\{\tau\}}\exp\left[-\beta H\{\tau\}+\beta\mu\sum_d\tau_d\right]. \tag{C1}$$

The thermal average of a functional $A\{\tau\}$ is given as

$$\langle A\rangle=Z^{-1}\sum_{\{\tau\}}A\{\tau\}\exp\left[-\beta H\{\tau\}+\beta\mu\sum_d\tau_d\right]. \tag{C2}$$

From Eqs. (C1) and (C2) one obtains

$$\left[\frac{\partial}{\partial\mu}\bigg|_{T,V}\right]\langle A\rangle=\beta(\langle NA\rangle-\langle N\rangle\langle A\rangle), \tag{C3}$$

where $N=\sum_d\tau_d$ is the number of interstitial particles. Choosing $A=\tau_a\tau_b$ one finds immediately from Eqs. (C3) and (2.29)

$$\sum_d\langle\tau_a\tau_b\tau_d\rangle_c=k_BT\left[\frac{\partial}{\partial\mu}\bigg|_{T,V}\right]\langle\tau_a\tau_b\rangle_c. \tag{C4}$$

Since the pressure p is given by

$$p(T,V,\mu)=-\partial J/\partial V\big|_{T,\mu},$$

where

$$J(T,V,\mu)=-k_BT\ln Z=-pV$$

is the grand canonical free energy, one can express Eq. (C4) as

$$\sum_d\langle\tau_a\tau_b\tau_d\rangle_c=V_{\rm cell}^{-1}k_BT\left[\sum_\gamma c_\gamma\right]\left[\frac{\partial}{\partial p}\bigg|_{T,V}\right]\langle\tau_a\tau_b\rangle_c. \tag{C5}$$

Here we have used $V=N_LV_{\rm cell}$, $N_H=n_HN_L$, and $\langle N\rangle=N_L\sum_\gamma c_\gamma$. Thus the pressure dependence of the two-point correlation function yields an integral of the three-point correlation function. In Fourier space we have for the cumulants c

$$\sum_\beta G^{(3,c)}_{\alpha-\beta,\alpha-\gamma}(0,\mathbf{q})=V_{\rm cell}^{-1}k_BT\left[\sum_\gamma c_\gamma\right]\times\left[\frac{\partial}{\partial p}\bigg|_{T,V}\right]G^{(2,c)}_{\alpha-\gamma}(\mathbf{q}). \tag{C6}$$

The pressure derivative of $G^{(2)}(\mathbf{q})$ determines $G^{(3)}(\mathbf{q}'=\mathbf{0},\mathbf{q})$. The antisymmetric part of the diffuse Huang scattering yields information which goes beyond that. According to Eq. (2.62) $C^{(3)}(\mathbf{q})$ probes $G^{(3)}(\mathbf{q}',\mathbf{q})$ even for $\mathbf{q}'\neq0$. Thus Eqs. (2.62) and (C6) represent independent checks for the three-point correlation function whereby Eq. (2.62) is the more sensitive one. In a modified form Eq. (C6) has been used by Egelstaff and coworkers[66] in order to check various approximation schemes for the three-point correlation function of simple, ordinary liquids.

In Eq. (C1) the Hamiltonian has the form of $H=H_{\rm int}+\sum_aV_a\tau_a$, where V_a is the binding energy at the interstitial site $\mathbf{s}_a$. Putting $H_{\rm int}=0$ one finds

$$Z=\prod_{a=1}^{N_H}\{1+\exp[-\beta(V_a-\mu)]\}$$

so that

$$c_\alpha=\{1+\exp[\beta(V_\alpha-\mu]\}^{-1}.$$

The results in Appendix A follow from

$$\left\langle\prod_{i=1}^n\tau_{a_i}\right\rangle=(-k_BT)^nZ^{-1}\partial^nZ/(\partial V_{a1}\times\cdots\times\partial V_{an}).$$

---

*New address: Institut für Physik, Universität Mainz, Postfach 3980, D-6500 Mainz 1, Federal Republic of Germany.

[1]W. Schilling, J. Nucl. Mater. **69&70**, 465 (1978).
[2]C. P. Flynn, *Point Defects and Diffusion* (Clarendon, Oxford, 1972).
[3]*Proceedings of the International Conference on Vacancies and Interstitials in Metals and Alloys,* edited by C. Abromeit and H. Wollenberger (Trans Tech, Switzerland, 1987).
[4]*Hydrogen in Metals Vols. I and II,* Vols. 28 and 29 of *Topics in Applied Physics,* edited by G. Alefeld and J. Völkl (Springer-Verlag, Berlin, 1978).
[5]L. van Hove, Phys. Rev. **95**, 249 (1954).
[6]B. Warren, *X-Ray Diffraction* (Addison-Wesley, Reading, 1969).
[7]H. Chen, R. J. Comstock, and J. B. Cohen, Annu. Rev. Mater. Sci. **9**, 51 (1979).
[8]B. Borie and C. J. Sparks, Acta Cryst. **A27**, 198 (1971).
[9]S. Dietrich and W. Fenzl, following paper, Phys. Rev. B **39**, 8900 (1989).
[10]J. D. Eshelby, in *Progress in Solid State Physics,* edited by F. Seitz and D. Turnbull (Academic, New York, 1956).
[11]R. O. Simmons and R. W. Baluffi, Phys. Rev. **117**, 52 (1960).
[12]K. Fischer and H. Hahn, Z. Phys. **172**, 172 (1963).
[13]K. Huang, Proc. R. Soc. London, Ser. A **190**, 102 (1947).
[14]M. A. Krivoglaz, *Theory of X-ray and Thermal Neutron Scattering from Real Crystals* (Plenum, New York, 1969).
[15]H. E. Cook, J. Phys. Chem. Solids **30**, 1097 (1969).
[16]P. H. Dederichs, J. Phys. F **3**, 471 (1973).
[17]H. Trinkaus, Z. Naturforsch. **28a**, 980 (1973).
[18]J. Peisl, J. Appl. Crystallogr. **8**, 143 (1975).
[19]J. Peisl, J. Phys. (Paris) Colloq. **37**, C7-47 (1976).
[20]P. Erhart and W. Schilling, Phys. Rev. B **8**, 2604 (1973).

[21]R. Kubo, J. Phys. Soc. Jpn. **17**, 1100 (1962).
[22]A. A. Maradudin and A. E. Fein, Phys. Rev. **128**, 2589 (1962).
[23]N. H. March, S. W. Wilkins, and J. E. Tiballs, Cryst. Lattice Defects **6**, 253 (1976).
[24]G. Alefeld, Phys. Status Solidi **32**, 67 (1969).
[25]H. Wagner and H. Horner, Adv. Phys. **23**, 587 (1974).
[26]*Physics of Superionic Conductors,* Vol. 15 of *Topics in Current Physics,* edited by M. B. Salamon (Springer-Verlag, Berlin, 1979).
[27]Y. Tsuchiya, S. Tamaki, and Y. Waseda, J. Phys. C **12**, 5361 (1979).
[28]V. F. Turchin, *Slow Neutrons* (Israel Program for Scientific Translations, 1963).
[29]G. E. Bacon, *Neutron Diffraction* (Clarendon, Oxford, 1975).
[30]S. W. Lovesey, *Theory of Neutron Scattering From Condensed Matter* (Oxford University Press, Oxford, 1984), Vols. 1 and 2.
[31]C. J. Sparks and B. Borie, in *Local Atomic Arrangements Studied by X-ray Diffraction,* edited by J. B. Cohen and J. E. Hilliard (Gordon and Breach, New York, 1966).
[32]H. Metzger, H. Behr, and J. Peisl, Z. Phys. B **46**, 295 (1982).
[33]G. A. Wolfe and B. Goodman, Phys. Rev. **178**, 1171 (1969).
[34]E. Nowak and P. H. Dederichs, Phys. Rev. B **25**, 875 (1982).
[35]A. Mookerjee and M. Yussouff, Phys. Rev. B **33**, 5414 (1986).
[36]M. J. Gillan and D. Wolf, Phys. Rev. Lett. **55**, 1299 (1985).
[37]E. Burkel, H. Dosch, J. Peisl, and P. Wochner, Verh. Dtsch. Phys. Ges. **23**, 39 (1988).
[38]D. Emin, Phys. Rev. B **3**, 1321 (1971).
[39]H. Dosch, B. Dorner, and J. Peisl, Phys. Rev. B **35**, 3069 (1987).
[40]J. Völkl and G. Alefeld, in *Diffusion of Hydrogen in Metals,* Ref. 4.
[41]K. H. Michel and J. Naudts, J. Chem. Phys. **68**, 216 (1978).
[42]E. Burkel, dissertation, Ludwig-Maximilians Universität München, 1982.
[43]V. Tewary, J. Phys. F **3**, 1515 (1973).
[44]G. Leibfried, and N. Breuer, *Point Defects in Metals I,* Vol. 81 of *Springer Tracts in Modern Physics* (Springer-Verlag, Berlin, 1978).
[45]H. J. Raveché, R. D. Mountain, and W. B. Street, J. Chem. Phys. **57**, 4999 (1972).
[46]J. L. Barrat, J. P. Hansen, and G. Pastore, Phys. Rev. Lett. **58**, 2075 (1987).
[47]A. Münster, *Statistical Thermodynamics* (Springer-Verlag, Berlin, 1956), p. 256.
[48]H. W. Jackson and E. P. Feenberg, Rev. Mod. Phys. **34**, 686 (1962).
[49]S. P. Ichimaru, Phys. Rev. A **2**, 494 (1970).
[50]L. Schäfer and A. Klemm, Z. Naturforsch. **34a**, 993 (1979).
[51]S. Dattagupta and L. A. Turski, Phys. Rev. Lett. **54**, 2359 (1985).
[52]S. Dietrich and H. Wagner, Z. Phys. B **36**, 121 (1979).
[53]E. Burkel, B. v. Guérard, H. Metzger, J. Peisl, and C.M.E. Ceyen, Z. Phys. B **35**, 227 (1979).
[54]W. Münzing, N. Stump, and G. Goeltz, J. Appl. Crystallogr. **11**, 588 (1978).
[55]T. Welberry, Rep. Prog. Phys. **48**, 1543 (1985).
[56]H. Jagodzinski, Prog. Cryst. Growth Charact. **14**, 47 (1987).
[57]D. Grasse, B. v. Guérard, and J. Peisl, Radiat. Eff. **66**, 21 (1982).
[58]D. Grasse, O. Kocar, S. C. Moss, and J. Peisl, Radiat. Eff. **66**, 61 (1982).
[59]P. Erhart, J. Nucl. Mat. **69&70**, 200 (1978).
[60]W. Mayer and J. Peisl, J. Nucl. Mater. **108&109**, 627 (1982).
[61]H. Metzger, J. Peisl, and J. Wanagel, J. Phys. F **6**, 2195 (1976).
[62]H. Metzger and J. Peisl, J. Phys. F **8**, 391 (1978).
[63]E. Burkel, W. Fenzl and J. Peisl, Philos. Mag. A **54**, 317 (1986).
[64]W. Fenzl and J. Peisl, Phys. Rev. Lett. **54**, 2064 (1985).
[65]W. Fenzl, dissertation, Ludwig-Maximilians Universität München, 1983.
[66]P. A. Egelstaff, D. I. Page, and C. R. T. Heard, J. Phys. C **4**, 1453 (1971).